Available online at www.joac.info

ISSN: 2278-1862

Journal of Applicable Chemistry

2014, 3 (2): 683-688

(International Peer Reviewed Journal)

Oxidation of Dipeptide Glycylglycine By PMS In Aqueous Medium And Comparison With Monomer Glycine: A Kinetic And Mechanistic Study

Prameela Kethavath[1], K Nagi Reddyand[3], P.Srinivas[2*]

1. Department of Chemistry, Dr. B. R. Ambedkar Open University- Hyderabad-33, **INDIA**
2. Department of Chemistry, Osmania University, Hyderabad-07, **INDIA**.
3. Department of Chemistry, CBIT, Hyderabad-75, **INDIA**

Email: Prameelachembraou@gmail.com, sripabba85@yahoo.co.in

Accepted on 1st March 2014

ABSTRACT

The kinetics of oxidation reactions of dipeptide Glycylglycine (GG) by Peroxomonosulphate (PMS)in aqueous medium, under the condition (PMS) << (GG) at different temperatures (313 – 323 K), to produce an aldehyde, and ammonia were studied. Perusal of the kinetic results showed that the first order dependence in [PMS] and fractional order dependence in [GG]. The effect of ionic strength and Acetonitrile (ACN) on rate was studied and thermodynamic parameters were also calculated. Michealis Menten type mechanism was proposed.

Keywords: The kinetics of oxidation reactions of dipeptide Glycylglycine, the effect of ionic strength, thermodynamic parameters.

INTRODUCTION

A peroxide compound contains an oxygen–oxygen single bond or the peroxide anion ($[O–O]^{2–}$)[1]. Peroxides can be roughly classified into organic and inorganic compounds. Whereas the inorganic peroxides have ionic, salt-like character, the organic peroxides are dominated by the covalent bonds. Peroxy compounds like PMS[2-3], Peroxodisulphate (PDS)[4-5], Peroxomonophosphate (PMP)[6], Peroxodiphosphate (PDP)[7] and organic peroxides[8-12] are economically and environmentally preferred for oxidation of organic compounds than conventional metal ions oxidants[2]. These reagents react with wide range of functional groups affecting an array of molecular transformations.

PMP and PMS can be considered as substituted hydrogen peroxide in which one of the hydrogen is replaced by an oxy anion group of phosphorous or sulphur. Even though PMP and PMS are more powerful oxidizing agents than the corresponding peroxodiacids ($H_4P_2O_8$ or $H_2S_2O_8$), sometimes they exhibit reducing properties similar to H_2O_2. PMS has been used as an oxidant in the study of kinetics of oxidation of organic compounds like carbonyl compound, alcohols and benzylic compounds [4-10]. PMS, which is structurally similar to peroxodisulphate (PDS), and has been shown to be a better oxidant than PDS in its reaction with halides[4,5]. PMS oxidizes the reductants to form sulphuric acid and the reaction involves

$$HSO_5^- + H_2O \rightarrow SO_4^{2-} + O_2^- + 2H^+$$

GG is a typical dipeptide which is the first member of dipeptide series. The oxidation of GG has been reported by a very few oxidants[13- 16]. GG undergo oxidation by two different routes based on the nature of the oxidant used and the reaction medium employed[17,18]. The first route is through C-C bond cleavage and second one is through N-H bond cleavage.

MATERIALS AND METHODS

GG (E.Merck, analytical grade) was purified by column chromatography and used in experiment. PMS obtained from Aldrich-West Hermann with highest purity and analytical grade used as received in stock solution. All other chemicals were of analytical grade.

Kinetics and Measurements: The kinetic studies were made under Pseudo-first order conditions with GG concentrations always greater than the concentration of PMS. The progress of the reaction was monitored by estimating the unreacted concentration of PMS by iodometrically using freshly prepared starch as an indicator.

Stoichiometry and product analysis: Under the conditions [PMS] >> [GG], the reaction was allowed to go to completion and the unreacted PMS was estimated iodometrically. It was found that one equivalent of GG required two equivalents of PMS and one equivalent of Gly needed one equivalent of PMS. The stoichiometric equation is given as

$$(^{+}NH_3)CH_2CONHCH_2COO^{-} + 2PMS \rightarrow CHOCONHCH_2COO^{-} + NH^{+}_4 + SO_4^{-2}$$

$$^{+}NH_3\ CH_2COO^{-} + PMS \rightarrow CHOCOO^{-} + NH^{+}_4 + SO_4^{-2}$$

Aldehyde formation was detected by chemical analysis 2,4-DNP reagent and TLC by comparing with standard, while ammonia was identified by Nessler's reagent.

RESULTS AND DISCUSSION

The kinetics of oxidation of GG by PMS was investigated at different [GG], conducted under the conditions [PMS] << [GG], the reaction was allowed to go for completion. The progress of the reaction was monitored by estimating the unreacted [PMS] at different intervals of time. The plots of log (a/a-x) (where 'a' and (a-x) corresponds to the concentration of PMS at zero time and at time't') Vs time were found to be linear passing through the origin fig-1 indicating first order dependence of rate in [PMS]. From the slops of such plots pseudo-first order rate constants (*k'*) evaluated were independent of [PMS], conforming the first order dependence in [PMS]. The rate increases with increasing in [GG].

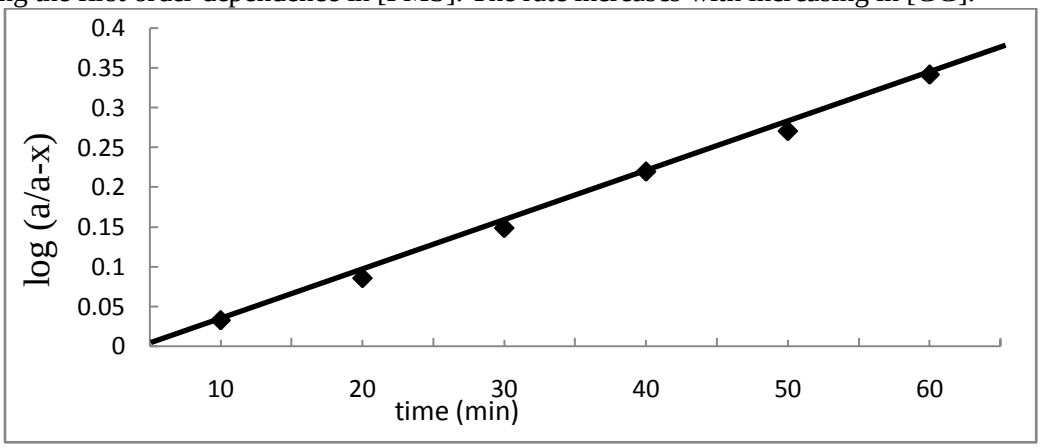

Fig.1. Oxidation of GG by PMS [PMS] =5 x 10^{-3} mol. dm^{-3} ; Temp = 313 K

The plot of log *k'* versus log [GG] is linear (r=0.99), with a slope of n=0.5 indicating a fractional order dependence of rate in [GG] Fig-2. No altering of order in GG further increasing [GG], the reaction obeying the Michealis-Menten kinetics (Table-1). The rate of oxidation of GG was decreased marginally with the

increase in ionic strength (addition of $NaClO_4$). The reaction rate was found to increase with increase in concentration of ACN content varied by the addition of 0-20% (v/v) ACN in the reaction medium. Blank experiment showed that ACN was not oxidised by PMS under experimental condition.

Table-1*:* Order in [GG] in the oxidation of [GG] by PMS in aqueous medium.[PMS] =5 x 10^{-3} mol. dm^{-3} **;** Temp = 313 K

10^2 x [GG] (mol dm^{-3})	k′x 10^3 min^{-1}	2+log[GG]	3+***logk′***
2.5	5.5	0.40	0.74
5.0	7.7	0.70	0.89
10.0	10.1	1.00	1.00
15.0	12.3	1.18	1.09
20.0	15.1	1.30	1.18

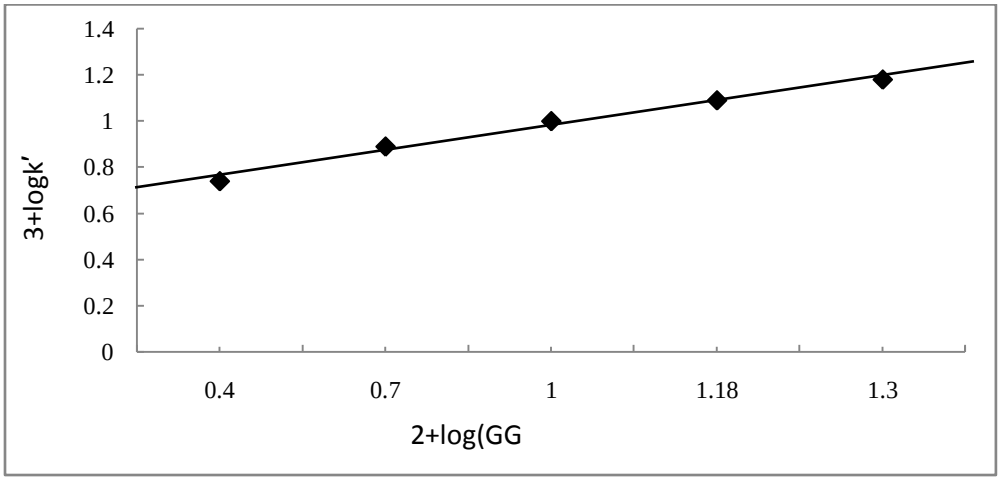

Fig.2 Effect of [GG] on *k′* in PMS-GG reaction [PMS] =5 x 10^{-3} mol. dm^{-3} ; Temp = 313 K

The kinetic study of the reaction is studied at different temperature from the range 313-323K. The substance concentration was changed at each temperature to Michealis-Menten kinetics. Activation parameters for the rate limiting step have been computed as follows:

Table-2: Activation parameters for the oxidation of GG by PMS.

Substrate	**E_a (kJ mol^{-1})**	**$\Delta H^{\#}$ (kJ mol^{-1})**	**$\Delta G^{\#}$ (kJ mol^{-1})**	**$\Delta S^{\#}$ (J mol^{-1} K^{-1})**
GG	27.2	24.6	107.8	-266
Glycine	13.1	10.5	133.8	-394

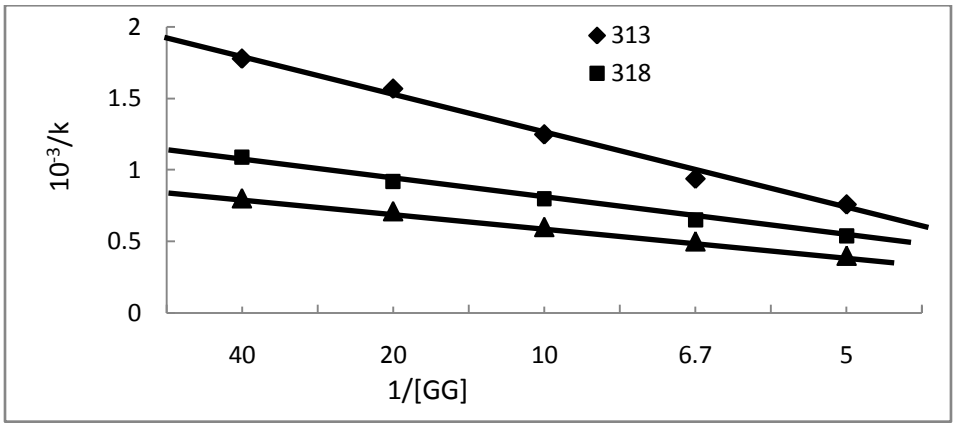

Peroxomonosulphuric acid (HO_OSO_3-H) has two ionizable protons, one is the sulphuric acid proton and the other is the hydrogen peroxide proton. The pKa value of the hydrogen peroxide proton[19] is 9.4. The oxidant peroxomonosulfate is a potential two equivalent oxidant and in most of the reaction usually the terminal peroxide oxygen atom is transferred to the reductants. In aqueous solution, PMS exists as a mixture of HSO_5^- and SO_5^{2-} due to the equilibrium (2).

$$HSO_5^- \underset{}{\overset{K_d}{\rightleftharpoons}} SO_5^{2-} + H^+ \quad \ldots\ldots\ldots\ldots\ldots (2)$$

The dissociation constant K_d is given in the literature as 4.0×10^{-10} M at 25°C [20]. Under the experimental conditions, $K_d / [H^+]$ value will be $<10^{-3}$ or even lesser and hence, all PMS will exist in the form of HSO_5^- . Therefore, HSO_5^- may be the active form of the oxidant under the experimental conditions. The kinetic scheme can be represented as in the following equations

$$GG + PMS^- \xrightarrow{k} \text{products} \ldots\ldots\ldots (3)$$

Equation (3) represents the interaction of the HSO_5^- with GG. Similar mechanisms were proposed in the oxidation of simple α-amino acids by PMS[8, 9].

In general, the reactions of peroxides are liable to acid catalysis. The higher reactivity of SO_5^{-2} than that of HSO_5^-may considered to be in favor of nucleophilic attack by the peroxide[10-12,21,22]. Based on this PMS can exist in two anionic forms, viz. PMS^- and PMS^{-2} depending upon the pH in aqueous solution. In the present kinetic study, under experimental pH condition PMS exist as PMS^-. Therefore, PMS^- can be assumed to reactive species in the oxidation of GG in aqueous medium.GG exists as Zwitterion, cation, anion and neutral molecule depending on the pH of the medium[23-28].Under the experimental conditions (pH= 3.42-5.89) zwitterionic form of GG is supposed to be the reactive species. Addition of olefinic monomer such as acrylamide or acrylonitrile did not induce polymerization confirming the absence of free radicals in the reaction mixture.

The first order dependence of rate on [PMS] and fractional order [GG] suggest that the reaction might occur via an adduct formation which dissociates in the slow rate determining step to give final products. A further support for the participation of ionic PMS species in the rate limiting step can be obtained from the rate enhancement with a decrease in the dielectric constant. On the basis of observed kinetic results, products of oxidation and above discussion, the reaction, under kinetic conditions, can be written as in

$(^+NH_3)CH_2CONHCH_2COO^- + PMS^- \rightarrow CHOCONHCH_2COO^- + NH^+_4 + SO_2^{-4}$…

…… (4)

The mechanism of oxidation of GG by HSO_5^- may be written as

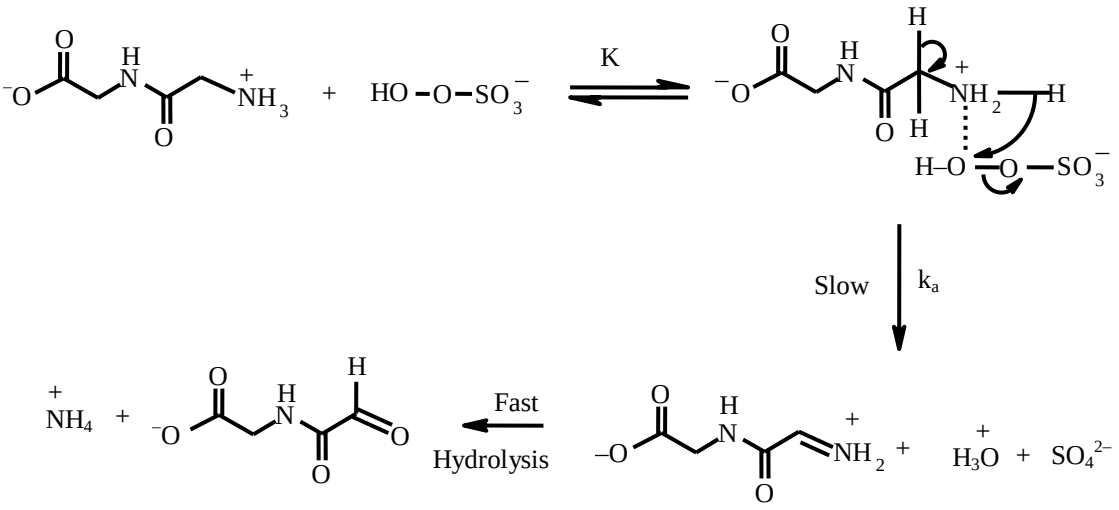

The oxidation products, namely an aldehyde (2-formylformamido aceticacid) and ammonia, suggest that the reaction center is the terminal amino group. The terminal carboxyl group is far away from the reaction center. Therefore, we can assume that the nature of the terminal carboxyl group, that is, charged or uncharged form, will have a least effect on the rate. This means the zwitterionic and the cationic form of GG will have the same rate. Only for simplicity, we have used only the zwitterionic form of GG in Eqs. (3). The rate equation for the disappearance of PMS can be given as following.

$$\text{Rate} = \frac{-d[PMS]}{dt} = \frac{kK[GG][PMS]}{1+K[GG]} \quad \ldots\ldots\ldots\ldots\ldots\ldots\ldots\ldots\ldots\ldots(5)$$

$$\frac{rate}{PMS} = \frac{kK[GG]}{1+K[GG]} \quad \ldots\ldots\ldots\ldots\ldots\ldots\ldots\ldots\ldots\ldots(6)$$

Reciprocal of equation (2) yields

$$\frac{[PMS]}{rate} = \frac{1}{Kk[GG]} + \frac{1}{k} \ldots\ldots\ldots\ldots\ldots\ldots\ldots\ldots\ldots\ldots(7)$$

A plot of 1/k′ Vs 1/[GG] is linear (r=0.99) with positive slope and intercept on Y-axis. This has been observed in the present investigation, supporting the proposed mechanism and Michealis –Menten[29] type kinetics. From the intercepts and slopes of [PMS]/rate Vs 1/[GG] plots at various temperatures k values are calculated (1.63 min^{-1} at 313K,2.89 min^{-1} at 318K and 4.12 min^{-1} at 323K) from which the activation parameters were calculated(Table-2) .

Comparison of rates of GG- PMS reaction with glycine(GLY)- PMS reaction under identical condition, revealed that the rate of oxidation is faster in case of glycine. The difference of reaction rates may be due to the (i) weaker electrostatic effects may occurs in the case of GG than Glycine (ii) Glycylglcine (pK_1 3.2 and pK_2 8.2) is weaker both as an acid and a base when compared to glycine (pK_1 2.4 and pK_2 9.8). Thus the oxidation of dipeptide GG is expected to be slower than the monomer.

APPLICATIONS

The present study will helps in the study of reactivity of organic and inorganic peroxides and peroxy derivatives with various biomolecules like proteins, nucleic acids (RNA & DNA), biopolymers like enzyme and carbohydrates etc. From which we can study the bonding interactions of peroxides with Biomolecules.

CONCLUSIONS

The rate of oxidation of GG and Glycine with PMS both shows first order dependence with respect to [PMS] and fractional order dependence with respect to [Substrate]. The rates were compared. The oxidation of GG and Glycine in the identical reaction conditions, the rate is slower in the case of GG than Glycine. It is may be due to weaker electrostatic interactions and functional group separation factors. Hence, the oxidation of GG is expected to slower than Glycine.

REFERENCES

[1] Nic, M.; Jirat, J.; Kosata, B., eds., "peroxides". IUPAC Compendium of Chemical Terminology (online ed) **2006**, 10, 1351.
[2] Karunakaran C &Palanisamy PN, *J Mol CatalA*, **2001**, 9, 172.
[3] P.Maruthamuthu and P.Neta, *J. Phys. Chem*.**1977**, 10, 81.
[4] Johnson R W & Edwards J O, *Inorg Chem*, **1966,** 5, 2073.
[5] Fortnum D H, Battallia C J, CoHen S R & Edwards J O, *J Am chemSoc*, **1960,** 82, 718.
[6] R.Viswamurthy and P.Maruthamuthu, *Oxidn communs*, **1981**, 2(1), 37.
[7] P.Maruthamuthu and M.Santappa, *Ind. J. Chem*.**1978**, 16A, 43.
[8] Ramchandran M S and Vivekanandam T S, *J. Chem. Soc perkin II*. **1984**, 1341.
[9] Ramchandran M S, Vivekanandam T S, and Mani Raj R P M, *J chem. Soc Perkin II.* **1984,** 1345.
[10] Pandurangan T and Maruthamuthu P. *Bull chem. Soc Japan*. **1981**, 54, 3351.
[11] Heinz G. O. Becker Organikum, Wiley-VCH. **2001**, p. 323.
[12] Egon Wiberg, Nils Wiberg, Arnold Frederick Holleman Inorganic Chemistry, Academic Press, **2001**, pp. 471.
[13] D.Krishna Bhat, B.Sheena Sherigara and B.Thimme Gowda, *Bull.Chem.Soc.Jpn*, **1996**, 41, 69**.**
[14] Amena Anjum and P. Srinivas, *Asian J. Chem.***2006**, 18, 1.
[15] T.Asha Iyengar and D.S.Mahadevappa, *Indian J.Chem*. **1992,** 31A, 752.
[16] K. Pramila, Birla Anjaiah and P.Srinivas ,*Asian Journal of Chemistry*, **2012**, 24(10) 4671-4674**.**
[17] T.Asha Iyengar and D.S.Mahadevappa, *Proc. Indian Acad.* **1993**, 63, 105.
[18] (a) B.T.Gowda and D.S.Mahadevappa, *J.Chem.Soc., Perkin Trans* .**1983**, 2, 323. (b) B.T.Gowda and B.S.Sherigara, *Indian J.Chem. Sect A,* **1987**, 26A, 930. (c) B.T.Gowda and R.V.Rao, Oxidn. Commun. **1988**, 149.
[19] D.L.Ball, and J.O. Edwards, J,Am. Chem. Soc. **1956**, 78, 1125**.**
[20] Project work submitted by J. Madhavan to university of Madras., doi:10.1016/j. solmat. **2005.**
[21] E.J.Hart, J.Am.Chem. Soc. **1961**, 83, 567**.**
[22] D.L.Ball, and J.O. Edwards, *J,Am. Chem. Soc.* **1956**, 78, 1125**.**
[23] Puttaswamy and Nirmala Vaz; *Bull. Chem.Soc. JPN*. **2003**, 76, 73**.**
[24] Sawyer, D. T. Superoxide Chemistry, McGraw-Hill. **2002,** 10. 1036**.**
[25] Michael Clugston; Rosalind Flemming. Advanced Chemistry, Oxford University Press, **2000,** p. 355**.**
[26] Foote, Christopher S.; Valentine, Joan S. Active oxygen in chemistry. Joel F. Liebman, A. Greenberg. Springer. **1995,** 153.
[27] Holleman, A. F.; Wiberg, E. "Inorganic Chemistry" Academic Press: San Diego, **2001.**
[28] Muller, F. L., Lustgarten, M. S., Jang, Y., Richardson, A. and Van Remmen, H. *Free Radic. Biol. Med.* **2007,** 43, 477**.**
[29] K J Laidler, Chemical kinetics (Pearson ed, Delhi) 3rd edition, **2008,** 412.

Available online at www.joac.info

ISSN: 2278-1862

Journal of Applicable Chemistry

2013, 2 (6): 1574-1580

(International Peer Reviewed Journal)

Oxidation of Dipeptide Glycylglycine by Chloramine-T in Aqueous Medium and Comparison with Monomer Glycine: A Kinetic and Mechanistic Study

Prameela Kethavath and P. Srinivas*

1. Department of Chemistry, Dr B R Ambedkar Open University-Hyderabad-33, **INDIA**
2. Department of Chemistry, Osmania University, Hyderabad-500 007, **INDIA**

Email: prameelachembraou@gmail.com,sripabba85@yahoo.co.in

Received on 9th October and finalized on 23rd October 2013

ABSTRACT

The kinetics of oxidation reactions of dipeptide glycylglycine(GG) by Chloramine-T(CAT) in aqueous medium to produce aldehyde, ammonia and carbon dioxide, under the condition [CAT] << [GG] at different temperatures (308-318 K) have been studied. The kinetics revealed that the fractional order dependence in [GG] and first order dependence in [CAT]. Michealis Menten type mechanism was proposed. Thermodynamic parameters have been evaluated. The rates of oxidation reactions were compared to that of the monomer glycine (Gly).

Keywords: Glycylglycine (GG), Glycine (Gly), Chloramine-T (CAT), Chloramine-B (CAB) and Acetonitrile (ACN).

INTRODUCTION

Proteins are essential constituents of all organisms. Most tasks performed by living cells require proteins. The variety of functions that perform is astonishing, and in which, oxidation of peptides and proteins is one major task. Oxidation of peptides and proteins involves various biochemical events ranging from normal metabolism to ageing and disease process[1]. Glycylglycine (GG) is a typical dipeptide which is the first member of dipeptide series. The oxidation of Glycylglycine has been reported by a very few oxidants[2,3]. GG undergo oxidation by two different routes based on the nature of the oxidant used and the reaction medium employed[4, 5]. The first route is through C-C bond cleavage resulting in decarboxylation and the second one is through N-H bond cleavage.

Chloramine-T (CAT) is N-haloarenesulfonamide derivative. The prominent members of these N-halo compounds, Chloramine-T (CAT), Bromamine-T (BAT), Chloramine-B (CAB) and Bromamine-B (BAB) have been employed as oxidants[6] in organic transformation and also for the determination of various organic, inorganic and pharmaceutical compounds. Among the N-haloarenesulfonamides, Chloramine-T (CAT) is gaining importance as strong oxidant and sometimes it act as vigorous oxidant[7]. It undergoes reduction to form 4-methyl benzenesulfonamide ($TsNH_2$) and the half cell reaction involves

$$TsNHCl + H^+ + 2\bar{e} \rightleftharpoons TsNH_2 + Cl^-$$

The redox potential for the couple Chloramine-T / $TsNH_2$ in aqueous medium was found to be >1.00 V at room temperature, indicating that Chloramine-T is considerably strong oxidant.

MATERIALS AND METHODS

GG (E.Merck, analytical grade) was purified by column chromatography and used in experiment. CAT and p-toluene sulphonamide obtained from Aldrich (U.S.A) with highest purity and analytical grade used in stock solution[8] of the oxidant preparation. All other chemicals were of analytical grade.

Kinetics and Measurements: The kinetic studies were made under pseudo-first order conditions with (CAT) << (GG) in aqueous medium. The progress of the reaction was monitored by estimating the unreacted (CAT) at different intervals of time. CAT content was estimated by iodometrically using a 1% solution of freshly prepared starch as an indicator. The concentration of CAT was calculated using the following stoichiometric equation.

$$p\text{-}MePhSO_2NClNa + 2I^- + 2H^+ \longrightarrow p\text{-}MePhSO_2NH_2 + I_2 + NaCl$$

Stoichiometry and product analysis: Under the conditions (CAT) >> (substrate) the reaction was allowed to go for completion. The unreacted (CAT) was estimated and based on the results, one mole of glycylglycine needed two moles of CAT and one mole of glycine needed one mole of CAT to get oxidised and the stoichiometric equation is given as

$$NH_2CH_2CONHCH_2COOH + 2\ p\text{-}MePhSO_2NClNa + 3H_2O \longrightarrow 2HCHO + 2\ p\text{-}MePhSO_2NH_2 + 2CO_2 + 2NH_3 + 2Na^+ + 2Cl^-$$

$$NH_2CH_2COOH + p\text{-}MePhSO_2NClNa + H_2O \longrightarrow HCHO + p\text{-}MePhSO_2NH_2 + CO_2 + NH_3 + Na^+ + Cl^-$$

Formaldehyde was detected by Chromo tropic acid[9] test, while ammonia was identified by Nessler's reagent[3], and carbon dioxide was detected by gas evolution apparatus. Formation of $TsNH_2$ identified by TLC, comparing with standard solution of pure $TsNH_2$.

RESULTS AND DISCUSSION

The kinetics of oxidation of GG by CAT was investigated at different (GG). Under the conditions of (GG) >> $[CAT]_0$, plots of log[a/a-x] (where 'a' and (a-x) corresponds to the concentration of Chloramine-T at zero time and at time 't') versus time were linear indicating a first order dependence of rate on $[CAT]_0$. Values of *k'*, calculated from these plots were independent of $(CAT)_0$, confirming the first order dependence on $(CAT)_0$ (fig 1). At constant $(CAT)_0$, the rate increases with increase in $(GG)_0$.

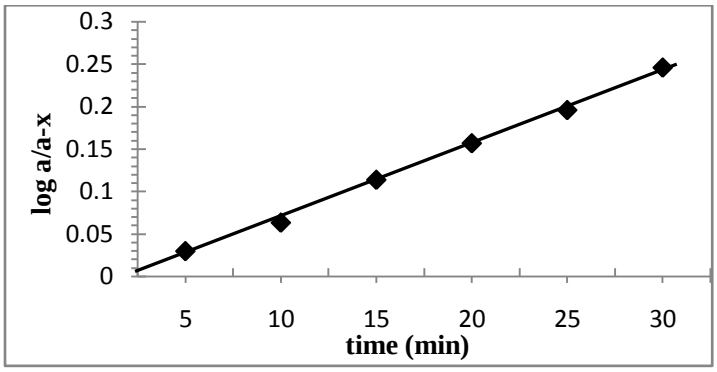

Fig. 1. Oxidation of glycylglycine by Chloramine-T.
[CAT]= 5 x 10^{-3} mol dm^{-3} **;** [GG] = 2.5 x 10^{-2} mol. dm^{-3}, T=308 K.

A plot of log *k′* versus log(GG) was linear (r=0.92,) with a slope (s=0.5) indicating a fractional order in (GG). Order in (GG) becomes zero as (GG) is increased further, obeying the Michealis-Menten kinetics (table-1). Increasing the [$HClO_4$], addition of $NaClO_4$ at fixed [H^+] and ionic strength did not affect the rate. The addition of p-CH_3-$PhSO_2NH_2$ also did not alter the rate of reaction. No significant change in rate was observed when the solvent composition of the medium was varied by the addition of 0-20% (v/v) Acetonitrile (ACN). Blank experiment shows that ACN was not oxidised by CAT under the experimental conditions.

Table-1: Order in [GG] in the oxidation of GG by CAT in aqueous medium; [CAT]= 5 x 10^{-3} mol dm^{-3};Temp = 308 K

10^2 x [GG] (mol dm^{-3})	k′x 10^3 min^{-1}	3+log[GG]	3+***logk′***
2.50	6.4	0.40	0.81
5.00	8.4	0.70	0.92
10.00	10.4	1.00	1.02
15.00	14.1	1.20	1.15
20.00	17.0	1.30	1.23

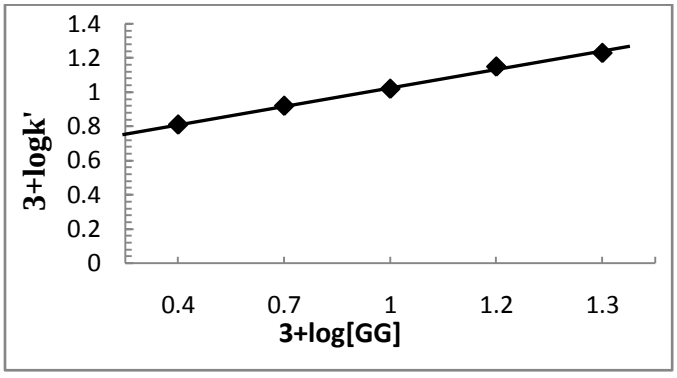

Fig 2. Effect of [GG] on k′ in CAT-GG reaction:
[CAT]= 5 x 10^{-3} mol dm^{-3}: Temp =308 K

The reaction was investigated at different temperatures in the range 308-318K. The substrate concentration was varied at each temperature to Michealis-Menten kinetics (Fig 3). Activation parameters for the rate limiting step have been computed as follows:

Substrate	E_a (kJ mol^{-1})	$\Delta H^{\#}$ (kJ mol^{-1})	$\Delta G^{\#}$ (kJ mol^{-1})	$\Delta S^{\#}$ (KJ mol^{-1})
GG	26.15	23.59	104.3	-262
Glycine	19.0	16.44	110.2	-259

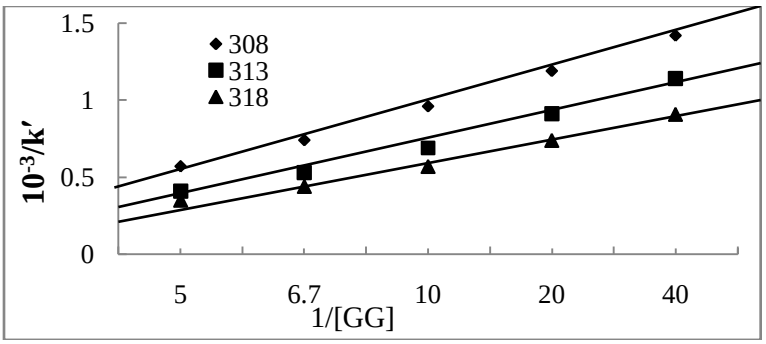

Fig 3. Plot 1/k′ versus 1/[GG] at rage 308-318K.

Absence of free radicals during the course of oxidation was confirmed when no polymerization was initiated with the addition of acrylonitrile solution to the reaction mixture. In aqueous solutions, Chloramine-T(CAT)[10] and its derivatives such as chloramine-B (CAB) and Bromamine-T act as electrolytes. Some of the important equilibria exhibited by CAT and CAB are represented by the following eqs.

$$ArSO_2NClNa \rightleftharpoons ArSO_2NCl^- + Na^+$$
$$ArSO_2NCl^- + H^+ \rightleftharpoons ArSO_2NHCl$$
$$2ArSO_2NHCl \rightleftharpoons ArSO_2NH_2 + ArSO_2NCl_2$$
$$ArSO_2NHCl^- + H^+ \rightleftharpoons ArSO_2NH_2Cl^+$$
$$ArSO_2NHCl + H_2O \rightleftharpoons ArSO_2NH_2 + HOCl$$
$$ArSO_2NCl_2 + H_2O \rightleftharpoons ArSO_2NHCl + HOCl$$
$$HOCl \rightleftharpoons H^+ + OCl^-$$
$$HOCl + H^+ \rightleftharpoons H_2OCl^+$$

CAT[11] exists in the following forms in aqueous medium viz., p-Me-Ph-SO_2NCl^-, (p-Me-Ph-$SO_2NH_2Cl)^+$, (p-Me-Ph-SO_2NCl_2), Cl^+, HOCl, and (H_2O^+Cl). In the present study, the possibility of ((p-Me-Ph-$SO_2NH_2Cl)^+$, Cl^+, H_2O^+Cl as the reactive species is ruled out, it is due to the rate decreases with increases in $[H^+]$ (table 2) in the oxidation of GG using Chloramine-T. ((p-Me-Ph-SO_2NCl_2) were to be the reactive species, the rate law would then predict a second order dependence of rate on (CAT) which is contrary to experimental observations. It suggests that Chloramine-T itself act as a reactive species in the oxidation of GG and glycine in aqueous medium.

Table 2. Effect of [$HClO_4$], [$NaClO_4$] and [p-TSA] on the rate of reaction, [CAT] =5 x 10^{-3} mol. dm^{-3} **;** [GG] = 2.5x 10^{-2} mol. dm^{-3}

[A] x 10^{-3} mol. dm^{-3}	A=[$NaClO_4$] 10^3 x k′ min^{-1}	A=[$HClO_4$] 10^3 x k′ min^{-1}	A=[p-TSA] 10^3 x k′ min^{-1}
00	6.4	6.4	6.4
1.0	6.7	5.8	6.3
1.5	6.6	4.6	6.3
2.0	6.8	3.9	6.5

Glycylglycine[12], like the amino acids, exists as zwitter ion, cation, anion and neutral molecule depending on the pH of the medium. Under the experimental conditions zwitterions form of glycylglycine is supposed to be the reactive species of glycylglycine, which gets further support from ionic strength effect. The inverse dependence of the reaction on $[H^+]$ suggests that the zwitter ion is reactive species taking part in the reaction. The absence of ionic strength effect on the rate limiting step. Based on the above observation, the mechanism of the reaction is outlined in Scheme 1:

$H_2N—CH_2—CONHCH_2COOH \rightleftharpoons H_3\overset{+}{N}—CH_2—CONHCH_2COO^-$ (X)

(X) + p-Me-$PhSO_2NHCl \overset{K}{\rightleftharpoons}$ X′

X′ $\xrightarrow[\text{Slow}]{k}$ X″

X″ + p-Me-$PhSO_2NHCl \rightleftharpoons$ Products (fast)

Scheme-1

Then rate is,

$$\text{Rate} = \frac{kK[GG][\text{CAT}]}{1+= \frac{-d[\text{CAT}]}{dt}K[GG]} \quad \ldots\ldots\ldots\ldots\ldots\ldots(1)$$

$$\frac{rate}{[CAT]} = \frac{kK[GG]}{1+K[GG]} \quad \ldots\ldots\ldots\ldots\ldots\ldots\ldots\ldots(2)$$

Reciprocal of equation (2) yields

$$\frac{[CAT]}{rate} = \frac{1}{kK[GG]} + \frac{1}{k} \ldots\ldots\ldots\ldots\ldots\ldots\ldots\ldots(3)$$

A plot of 1/k′ versus 1/[GG] is linear (r=0.97) and from the intercept of the reciprocal plot, the value of k was computed. The rate of reaction was fractional order in $(GG)_0$ and so Michealis –Menten[13] type kinetics were followed by varying the $[substrate]_0$ over the range of temperature (308-318K) and the values of 10^4k was computed as 5.58, 7.14 and 9.91 min^{-1} at 308, 313 and 318K respectively.

The rate of oxidation of GG by CAT was compared with that of glycine by CAT under identical experimental conditions and it was found that the rate of oxidation of GG is shows slightly slower than glycine (table 3). The difference of reaction rates may be due to the (i) increased distance between the functional groups, which result in weaker electrostatic effects (ii) glycylglycine (pK_1 3.2 and pK_2 8.2) is weaker both as an acid and a base when compared to glycine (pK_1 2.4 and pK_2 9.8). Thus the oxidation of dipeptide glycylglycine is expected to be slower than the monomer.

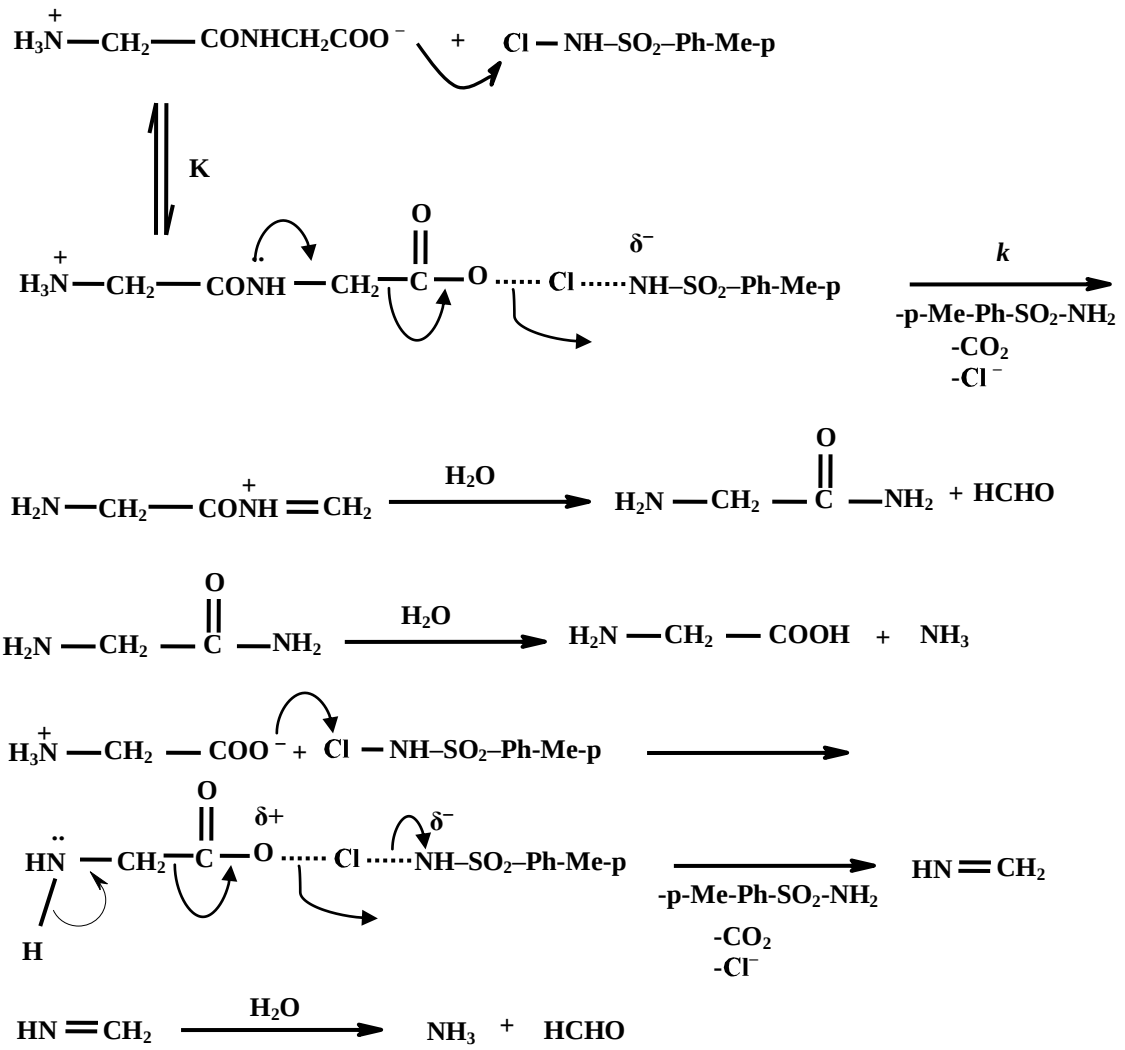

Scheme-2

Table 3. Comparison of rates of oxidation of GG and Gly by CAT: [CAT]= 5 x 10^3 mol dm^{-3}, Temp = 308 K

10^2 x [GG] (mol dm^{-3})	k′x 10^3 min^{-1}	10^2 × [Glycine] (mol-dm^{-3})	10^3 × k′(min^{-1})
2.50	6.4	2.5	10.0
5.00	8.4	5.0	13.1
10.00	10.4	10.0	16.5
15.00	14.1	15.0	19.8
20.00	17.0	20.0	21.9

Scheme 2 depicts the probable mode of oxidation of GG by CAT in aqueous medium over a range of temperature (308-318K). The Zwitter ion of GG is attacked at the carboxylate end by halogen species yielding an intermediate, X′. The intermediate, X′ with the liberation of CO_2, Cl^- and $TsNH_2$ forms another intermediate, X″ which ultimately gives the products observed.

APPLICATIONS

This report is helpful for the study of oxidation of amino acids, peptides and proteins with a radical and non radical reactive species as well as an exploration of the significance of reactive species in the atmosphere, disinfection process and environment remediation.

CONCLUSIONS

The rate of oxidation of glycine and glycylglycine by CAT were compared under identical experimental conditions and it was found that the rate of oxidation of glycylglycine is slower than that of glycine. The change is due to the increased distance between the functional groups and consequently weaker electrostatic effects[14]. Hence, the oxidation of glycylglycine is expected to be slower than that of glycine.

REFERENCES

[1] Barbara S. Berlett and Earl R.Stadtman., *The Journal of Biological Chemistry*, **1997**, 272, 20313-20316.
[2] (a) D.Krishna Bhat, B.Sheena Sherigara and B.Thimme Gowda, *Bull.Chem.Soc.Jpn.* **1996**, 69, 41.
(b) Amena Anjum and P. Srinivas, *Asian J. Chem.*, **2006**, 18, 1.
[3] (a) T.Asha Iyengar and D.S.Mahadevappa, *Indian J.Chem*. **1992**, 31A, 752.
(b) K. Pramila, Birla Anjaiah and P.Srinivas Asian Journal of Chemistry; **2012**, 24, 10, 4671-4674.
[4] T.Asha Iyengar and D.S.Mahadevappa,, *Proc. Indian Acad,* **1993**., 63, 105.
[5] (a) B.T.Gowda and D.S.Mahadevappa, *J,Chem.Soc., Perkin Trans* **1983**, 2, 323. (b) B.T.Gowda and B.S.Sherigara, *Indian J.Chem. Sect A*, **1987**, 26A, 930. (c) B.T.Gowda and R.V.Rao, *Oxidn. Commun.,* **1988**, 149.
[6] N.K.Mathur and C.K.Narang, 'determination of organic compounds with N-bromosuccinimide and allied reagents", academic press, London, **1975**.
[7] R.Filler, *Chem. Rev*, **1963,** 63, 21.
[8] M S Ahmed & D S Mahadevappa, *Talanta*, **1980**, 27, 669.
[9] D K Bhat, B S Sherigara and B T Gowda, *Bull. Chem. Soc. (Japan)*, **1996**, 69, 41.
[10] R Ramachandrappa, Diwya and Pushpa Iyengar., *RJPBCS*, **2012**, 3 (1), 835.
[11] V. S. Kiranmai Kolachana, Kishore Cholkar, Waseem M. Kayani, Gilles K. Kouassi, R.V. Jagadeesh, Netkal M. Made Gowda, *American Journal of Organic Chemistry* **, 2012,** 2(1), 18,
[12] L F Fieser & M Fieser, *Organic chemistry (D C Heath, Boston),* **1958**, 417.
[13] K J Laidler, Chemical kinetics (Pearson ed, Delhi), **2008**, 412.
[14] D.W.Urray, D. Channegowda, T.M. Parker, C. H. Luan, M. C. Reid, C. M. Harris, G.Pattanaik and D.R.Harris, *Biopolymers*, **1992**, 32, 1243.

Asian Journal of Chemistry; Vol. 31, No. 12 (2019), 2897-2902

ASIAN JOURNAL OF CHEMISTRY

https://doi.org/10.14233/ajchem.2019.22334

Microwave Assisted Synthesis and Optical Properties of Highly Fluorescent N-Doped Carbon Dots

D. KOTESWARARAO[1,2], B. RAJKUMAR[3], K. PRAMEELA[2], K. ASHOK[4] and G. SRIDEVI[4,*]

[1]Department of Chemistry, Jawaharlal Nehru Technological University, Hyderabad-500085, India
[2]Department of Chemistry, Dr. B.R. Ambedkar Open University, Hyderabad-500033, India
[3]Department of Chemistry, Osmania University, Hyderabad-500007, India
[4]Dhruvtara Chemicals Pvt. Ltd., #G1 Seven Hills Moon Apts, Snehapuri Colony, Hyderabad-500076, India

*Corresponding author: E-mail: drsridevikalyani@gmail.com

Received: 16 June 2019; *Accepted*: 13 August 2019; *Published online*: 16 November 2019; AJC-19638

Herein, a rapid microwave assisted solid state method is reported for the synthesis of highly fluorescent N-doped carbon dots (NCDs) using citric acid as carbon source and guanidine hydrochloride as N-dopant. Synthetic parameters such as microwave power, irradiation time and reactants ratio were optimized to produce high quality N-doped carbon dots. The N-doped carbon dots were well characterized using transmission electron microscopy (TEM), X-ray diffraction (XRD), SEM-EDS, FTIR, UV-visible and fluorescence spectroscopies. N-Doped carbon dots exhibited bright emission with a quantum yield of 11 %. Detailed study of their optical properties revealed their excellent property of resistance to photo bleaching, high ionic strength and solution pH. Further they exhibited excitation dependent emission behaviour, high aqueous solubility and a long shelf life of 60 days. This strong fluorescence emission combined with high stability make N-doped carbon dots a promising fluorescent probe for wide range of applications.

Keywords: N-Doping, Carbon dots, Citric acid, Guanidine hydrochloride, Fluorescence.

INTRODUCTION

Luminescent carbon dots (CDs) serendipitously discovered in the year 2004, have grabbed the attention of many research groups with their spectacular properties [1]. They are fool proof and robust materials with unique, versatile and novel properties such as chemical inertness, superior stability against photo bleaching, biocompatibility and low cytotoxicity which made them find wide applicability in various fields [2,3]. They are best known for their strong and stable fluorescence ability. These are the nanoparticles of carbon and considered as raising star of the carbon nanomaterials family with sub 10 nm of diameter. Since their first discovery, several researchers came up with a wide variety of approaches ranging from laser ablation, arc discharge, thermal and electrochemical treatments to ultrasonication, hydrothermal and microwave treatments for the production of carbon dots (CDs) [4-6]. Furthermore, application of CDs to numerous areas including biomedicine, biomedicine delivery, sensing, catalysis and optoelectronic conversion were also widely explored [7-9]. Carbon dots (CDs) can be viewed as promising alternatives to traditional fluorescent substances with their superior features of good water dispersibility, non-toxic nature, and high tolerance to photo bleaching [10].

Although considerable progress has been made towards the production and usage of CDs to diversified fields, much more research needs to be focused on synthesizing CDs in ways of overcoming the major drawbacks like poor fluorescence quantum yields [7,11]. Doping of heteroatoms particularly N and S into the carbon core is considered to be promising in this regard. Currently, researchers are making several attempts in developing novel strategies for the production of improved CDs with doping [11]. In most of the studies, hydrothermal treatment is successfully applied for CDs production by employing many natural resources, waste materials and various organic small molecules [12]. However, hydrothermal treatments generally require long reaction times. Recently, usage of microwave radiation for the synthesis of carbon dots (CDs) have gained much attention and diverse starting materials including small organic molecules like hydrocarbons, acids, esters and natural resources [6,13]. Microwave radiation assisted fabri-

cation offers advantages such as operational simplicity, cost effectiveness and a rapid reaction times and avoids the traditional harsh treatments like strong acids, elevated temperatures, and lengthy reaction times [14].

Here in this work, we report a simple microwave assisted production of N-doped carbon dots (NCDs) with fluorescent quantum yield as high as 11 %. Citric acid is used as carbon source and guanidine hydrochloride as dopant and various synthetic conditions like microwave power, irradiation time and mole ratio of reactants are optimized. The as-fabricated NCDs were systematically characterized by various analytical techniques and their optical properties are studied.

EXPERIMENTAL

Citric acid and guanidine hydrochloride were procured from S.D. Fine Chemicals Ltd. Mumbai, India. All the chemicals and reagents used in the present study are of analytical grade and used without further purification. Double distilled water was used throughout the study.

Synthesis of N-doped carbon dots (NCDs): Appropriate amounts of citric acid and guanidine hydrochloride (mole ratio of 1:2) were placed in an agate mortar and grounded into a uniform powder. Then the mixture was taken in a glass vial, placed in a domestic microwave oven and heated at 500 W for 5 min followed by the addition of 10 mL of double distilled water to obtained a char like material. The obtained brown coloured solution containing N-doped carbon dots (NCDs) is then centrifuged and filtered to remove large particles. Unreacted reactant molecules and other small molecules were removed by dialysis (MWCO 3500Da).

Fluorescence spectral measurements were carried out using a JASCO spectrofluorometer (FP-8500) set with excitation and emission slit widths at 2.5 nm. UV-visible spectral studies were conducted on Shimadzu UV-VIS-NIR 3600 spectrophotometer. Transmission electron microscopy (TEM) images were acquired on a JEOL 3010 microscope operating at 200 kV by drop casting an appropriate dilution of NCDs aqueous solution onto the carbon-coated copper grids. Fourier Transform Infrared (FT-IR) spectrum was recorded on Shimadzu IR Prestige-21 spectrophotometer. X-ray diffraction (XRD) patterns of NCDs were obtained using an X'pert Pro powder X-ray diffractometer (Netherlands) with Cu Kα radiation, λ = 1.5406 Å.

Quantum yield calculation: Quantum yield (QY) of N-doped carbon dots (NCDs) was determined by comparing the integrated fluorescence intensities and absorbance values with those of reference compound (quinine sulfate). Quinine sulfate (Φ = 0.54) was dissolved in 0.1M H_2SO_4 (η = 1.33) and the NCDs were present in double distilled water (η = 1.33). To avoid inner filter effect, absorbance values were kept less than 0.1. Finally, quantum yields were calculated by employing the following equation:

$$\Phi = \Phi_R \frac{I}{I_R} \times \frac{A_R}{A} \times \frac{\eta^2}{\eta_R^2}$$

where Φ is the quantum yield, I is the recorded integrated emission intensity, A is the absorbance at excitation wavelength, and η is the refractive index. The subscript R denotes reference compound (quinine sulfate).

RESULTS AND DISCUSSION

Synthesis of N-doped carbon dots (NCDs): In this work, a simple, green, microwave assisted solid state synthesis of N-doped carbon dots is reported. Citric acid is used as carbon source and guanidine hydrochloride as dopant. Synthetic conditions such as microwave power, heating time and reactants ratio were optimized by taking quantum yield of the produced N-doped carbon dots (NCDs) as a parameter. Firstly, mole ratio of reactants was optimized by keeping the microwave power at 500 W and heating time at 5 min. As shown in Fig. 1a, the mole ratio of 1:2 (citric acid to guanidine hydrochloride) resulted NCDs with high quantum yield.

Similarly, microwave power was also optimized by keeping other conditions constant. As shown in Fig. 1b with increase in the microwave power from 180 to 500 W, the quantum yield also increased. However, further increase in microwave power resulted in a drastic decrease in the quantum yield and water insoluble char like product was obtained at a microwave power above 900 W. Furthermore, microwave irradiation time was optimized by keeping other parameters constant. Increase in the irradiation time from 1 min to 5 min resulted in a clear increase in the quantum yield and reached the maximum value (Fig. 1c). However, at higher irradiation time, NCDs with relatively low quantum yield were obtained. This can be ascribed to the fact that increased reaction times will lead to the over carbonization of the formed carbon dots which in turn would lead to the decrease in the quantum yield [15]. Thus, the optimized synthetic conditions are 1:2 mole ratio of citric acid and guanidine hydrochloride, microwave power of 500 W and irradiation time of 5 min.

TEM analysis: The structure, morphological features and size distribution of NCDs obtained under optimal synthetic

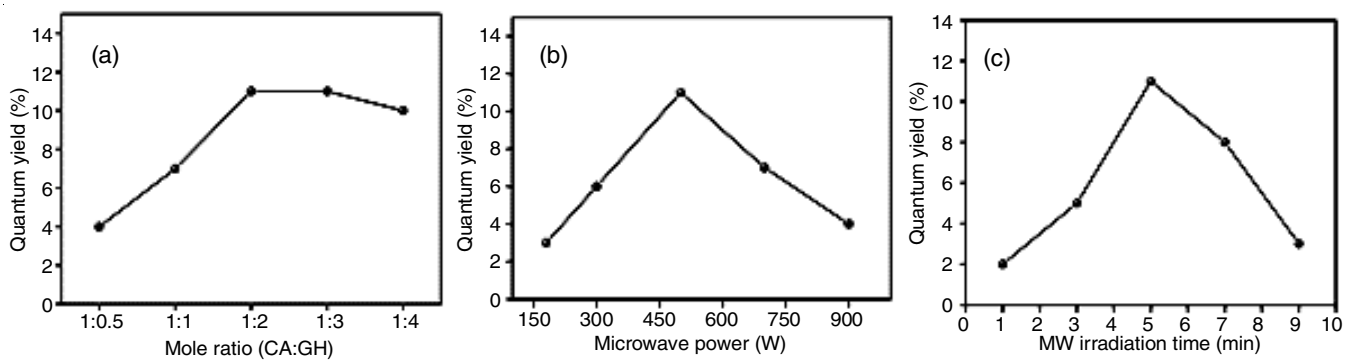

Fig. 1. Optimization of synthetic conditions: QY as a function of (a) mole ratio (b) microwave power and (c) microwave irradiation time

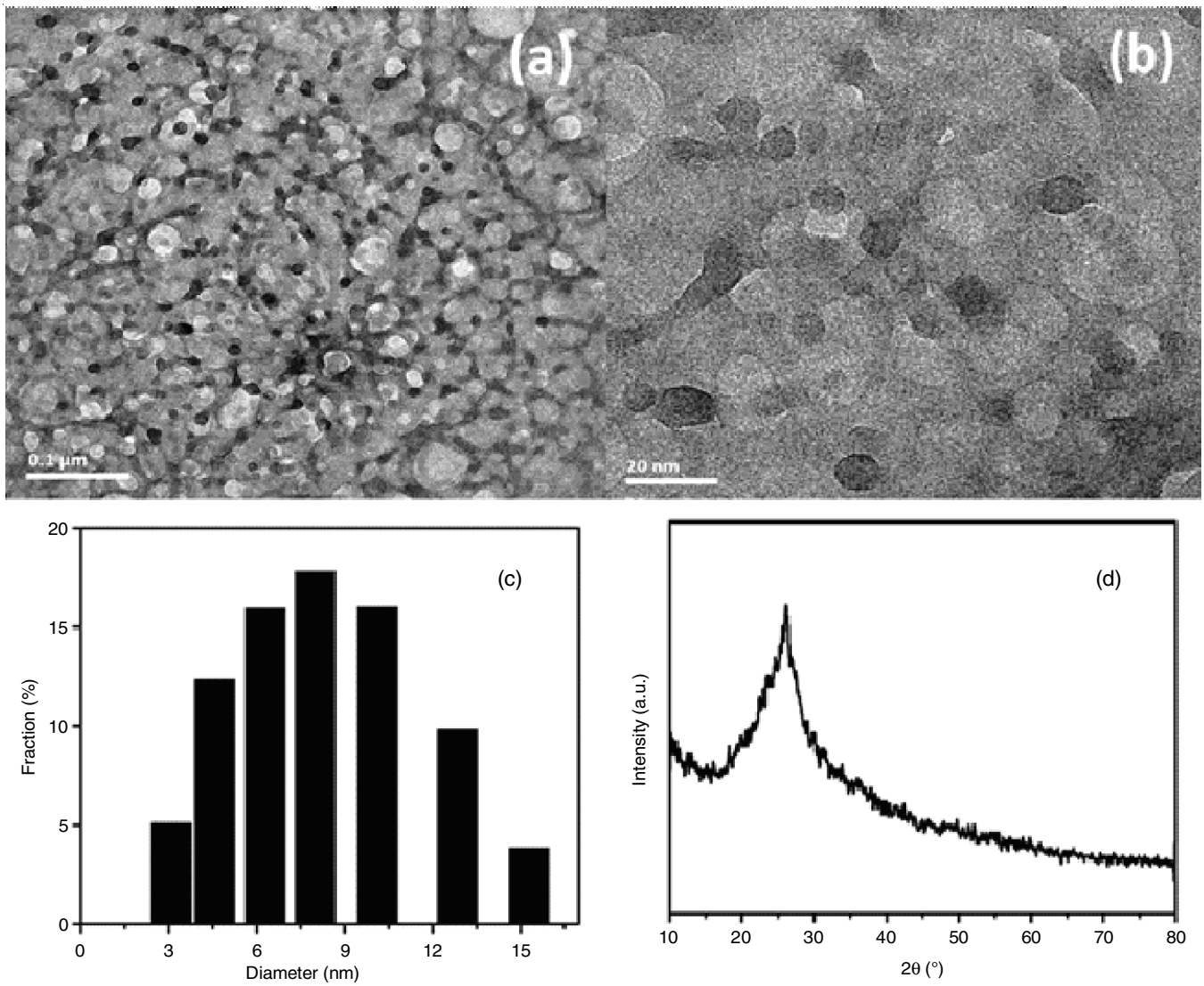

Fig. 2. TEM images of NCDs (a) low magnification (b) high magnification and (c) corresponding particle size distribution (d) powder XRD pattern of NCDs

conditions were studied by using TEM analysis. TEM image shown in the Fig. 2a clearly revealed the spherical morphology of NCDs and the particles were well separated from each other without undergoing any agglomeration.

Corresponding size distribution histogram is shown in Fig. 2b suggested the size of NCDs ranging from 3 to 15 nm with an average diameter of 8 nm. Powder XRD patterns of NCDs (Fig. 2c) exhibited a single broad peak centred at 2θ = 26.2º indexed to the (002) lattice spacing of graphitic carbon indicating the graphite like structure of NCDs [15]. The interlayer spacing d (0.37 nm) is larger than that of graphite (0.34 nm) suggesting the incomplete graphitization or amorphous nature and can be attributed to the existence of polar functional groups on the surface [16].

SEM-EDS analysis: The chemical composition of NCDs is evaluated by using SEM-EDS analysis. As shown in Fig. 3, the NCDs are composed of carbon (56.57 %), nitrogen (14.55 %) and oxygen (28.88 %).

FTIR analysis: In the FTIR spectrum (Fig. 4), the broad vibration band in the range of 3500-3200 cm^{-1} can be ascribed to the characteristic -OH and -NH stretching vibrations. The

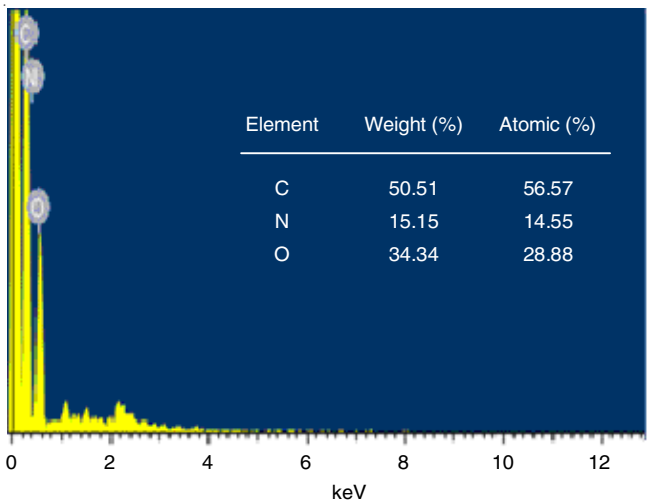

Fig. 3. SEM-EDS analysis of N-doped carbon dots

peak at 1643 cm^{-1} represents the carbonyl stretching, while the peaks in the range of 1600 to 1400 cm^{-1} can be assigned to C=C stretching vibrations of polycyclic aromatic hydrocarbons

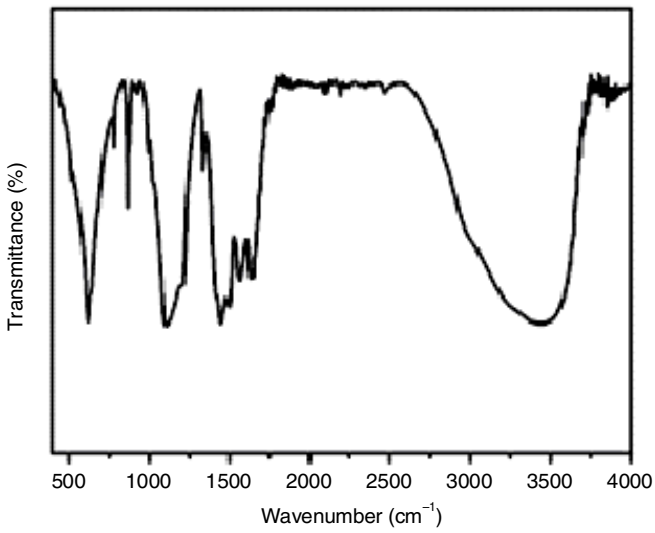

Fig. 4.FT-IR spectra of N-doped carbon dots

indicating the presence of sp^2 hybridization. Further, the peaks at 1211 and 1100 cm^{-1} can be ascribed to the stretching and bending vibrations of C-O bonds in carboxyl groups. These results manifest that the NCDs comprise multiple functional groups like -OH, -COOH and NH on their surface which makes them highly soluble in water. Further, these functional groups can act as linkers for the attachment of biomolecules to serve NCDs as nano-carriers [17].

Optical properties: UV-visible and fluorescence spectroscopic techniques were employed to study the optical properties of NCDs. Under day light, aqueous solution of NCDs appeared transparent and pale yellow coloured whereas the same solution exhibited bright blue emission under 360 nm UV lamp (Fig. 5). The absorption spectra and emission spectra of NCDs aqueous solution at ambient conditions is presented in Fig. 5. In the absorption spectra, two poorly resolved bands can be observed at around 290 and 370 nm. These bands might be aroused from the π-π^* transition of carbogenic core and n-π^* transition of heteroatomic surface functionalities, respectively [10]. The emission spectra of NCDs presented a strong peak

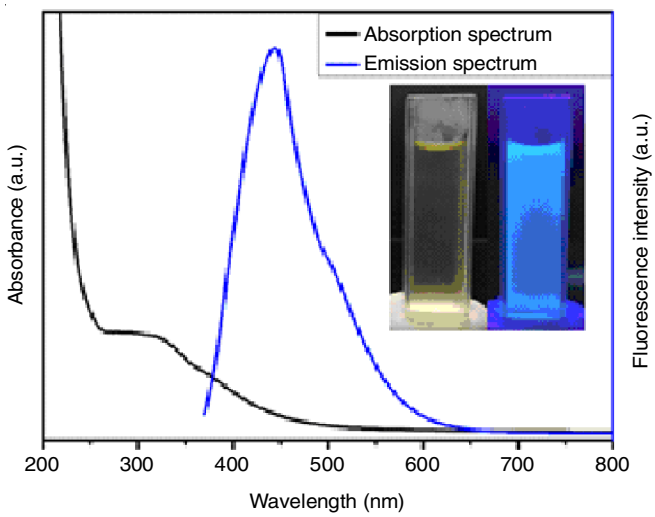

Fig. 5. Absorption and fluorescence emission spectra of NCDs, inset: photographs of NCDs aqueous solution exposed to day light (left) and 360 nm UV light (right)

centred at 445 nm (λ_{ex} = 360 nm) with a stoke shift of 85 nm and full width at half maximum (FWHM) of 90 nm. These observations are well in accordance with the previous reports.

Fluorescence spectra: The emission spectra of NCDs was recorded at various excitation wavelengths. As shown in Fig. 6, the emission intensity increased with increase in the excitation wavelength from 300 to 360 nm. However, further increase in the excitation wavelength resulted in a clear decrease in the emission intensity. Furthermore, with increase in the excitation wavelength from 300 to 480 nm a clear red shift in the emission peak position from 437 nm to 535 nm was observed. These results suggest that the CDs do not obey Kasha's rule which suggest that the emission peak position of a fluorophore will not depend on the excitation wavelength. This kind of excitation dependent emission nature is considered as the characteristic feature of CDs and makes them as fluorescent probe for multicolour imaging [18]. The origin of this excitation dependent nature is either due to the optical selection of differently sized nanoparticles (quantum effect) and/or different emissive traps on their surface or some other mechanism altogether, is presently unresolved and a matter of debate among the scientific community [1]. Quantum yield of NCDs determined by using quinine sulphate as reference compound is found to be 11 %, which is higher than several previous reports [19-21]. The reason for this higher quantum yield can be attributed to the doping with nitrogen element [22].

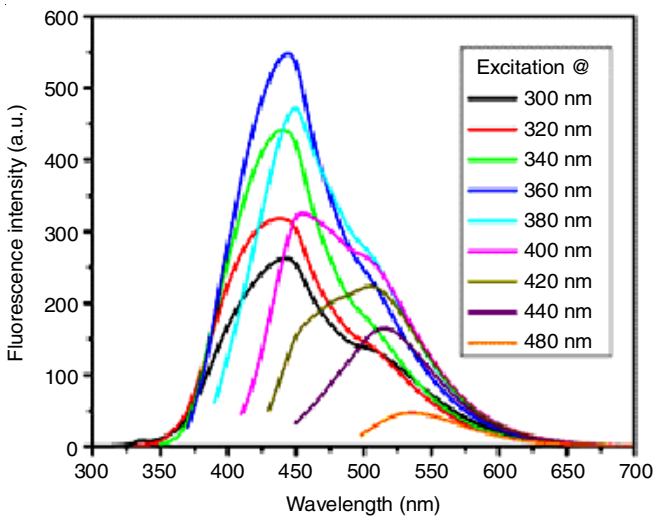

Fig. 6. Emission spectra of NCDs at different excitation wavelengths

Fluorescene stability: It is well known that the emission intensity of many fluorescent probes will be disrupted by complex environmental conditions. Hence to test the ability of NCDs to be used as a fluorescent probe for various practical applications, their fluorescence stability was tested under diverse conditions. Firstly, we have examined the effect of ionic strength by recording the emission spectra of NCDs at various KCl concentrations. As shown in Fig. 7a, only a slight decrease in the emission intensity appeared even at a high KCl concentration of 2M. This verifies the tolerance of NCDs to high ionic conditions and further extends their applicability to similar ion rich biological environments [23]. As shown in Fig. 7, solution pH has some significant effect on the emission intensity

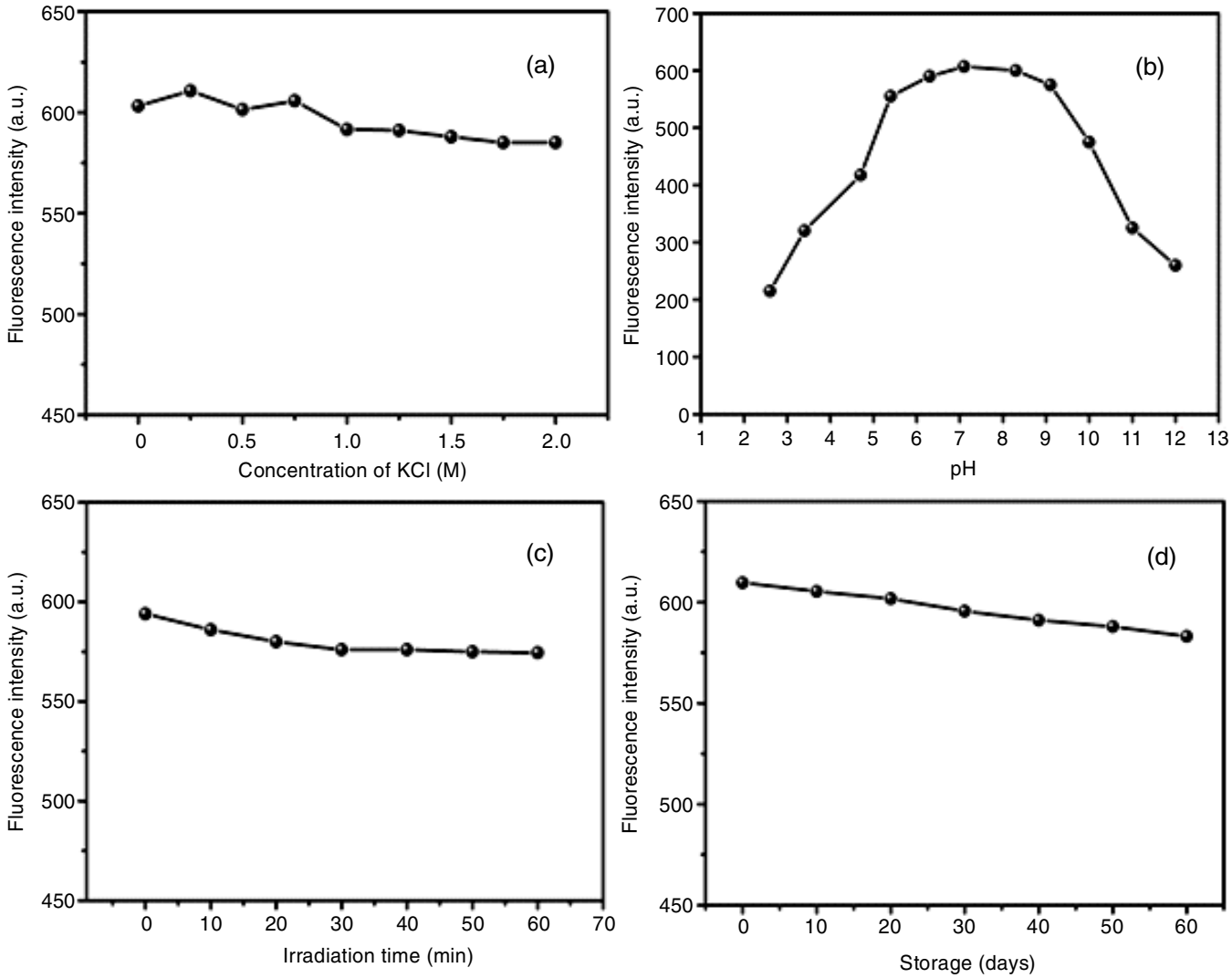

Fig. 7. Effect of (a) concentration of KCl (b) solution pH (c) UV light exposure time and (d) storage on the fluorescence intensity of NCDs (λ_{em} = 445 nm and λ_{ex} = 360 nm)

but fortunately the emission intensity was high and remained almost constant in the pH range of 5 to 9 which is the common pH range of many environmental and biological samples.

Strong acidic and basic conditions cause some severe protonation and deprotonations on the surface of NCDs which might lead to the aggregation of nanoparticles and result in decreased fluorescence emission [24]. Photostability or resistance to photo-bleaching is an important characteristic for a fluorophore to be used in various applications ranging from imaging to optoelectronics. Photostability studies were performed by continuously irradiating the aqueous solution of NCDs under 360 nm UV lamp for 1 h. No significant decrease in the emission intensity was observed even after 1 h of exposure (Fig. 7c), indicating the superior photo stability of NCDs. Furthermore, the shelf life of NCDs aqueous solution was evaluated by storing it under ambient conditions. Again, no substantial decrease in the emission intensity was observed even after storing for 60 days and the solution remained clear, implying the great stability and long shelf life of NCDs (Fig. 7d). All these results suggested that the produced NCDs are highly stable and can serve as excellent candidates for diverse applications.

Conclusion

To summarize, we have successfully demonstrated a simple microwave assisted method for the production of N-doped carbon dots with quantum yield as high as 11 %. The synthesized NCDs contain various polar surface functionalities which impart favourable aqueous solubility. N-doped carbon dots (NCDs) displayed excitation dependent emission behaviour which is crucial in multicolour imaging. Further, NCDs exhibited strong fluorescence emission which is stable to various environmental conditions such as high ionic strength, solution pH and continuous irradiation. Furthermore, they showed long shelf life of 60 days. All these properties make NCDs an excellent fluorescent probe for wide variety of applications ranging from bioimaging and chemical sensing to optoelectronic devices.

CONFLICT OF INTEREST

The authors declare that there is no conflict of interests regarding the publication of this article.

REFERENCES

1. S.N. Baker and G.A. Baker, *Angew. Chem. Int. Ed.*, **49**, 6726 (2010); https://doi.org/10.1002/anie.200906623.
2. S.Y. Lim, W. Shen and Z. Gao, *Chem. Soc. Rev.*, **44**, 362 (2015); https://doi.org/10.1039/C4CS00269E.
3. J. Wang and J. Qiu, *J. Mater. Sci.*, **51**, 4728 (2016); https://doi.org/10.1007/s10853-016-9797-7.
4. O. Kargbo, Y. Jin and S.-N. Ding, *Curr. Anal. Chem.*, **11**, 4 (2014); https://doi.org/10.2174/15734110106661410101602 17.
5. K. Dimos, *Curr. Org. Chem.*, **20**, 682 (2016); https://doi.org/10.2174/1385272819666150730220948.
6. P. Zuo, X. Lu, Z. Sun, Y. Guo and H. He, *Mikrochim. Acta*, **183**, 519 (2016); https://doi.org/10.1007/s00604-015-1705-3.
7. W. Liu, C. Li, Y. Ren, X. Sun, W. Pan, Y. Li, J. Wang and W. Wang, *J. Mater. Chem. B Mater. Biol. Med.*, **4**, 5772 (2016); https://doi.org/10.1039/C6TB00976J.
8. Z.L. Wu, Z.X. Liu and Y.H. Yuan, *J. Mater. Chem. B Mater. Biol. Med.*, **5**, 3794 (2017); https://doi.org/10.1039/C7TB00363C.
9. A.J. Wang, H. Li, H. Huang, Z.S. Qian and J.J. Feng, *J. Mater. Chem. C Mater. Opt. Electron. Devices*, **4**, 8146 (2016); https://doi.org/10.1039/C6TC02330D.
10. R. Bandi, R. Dadigala, B.R. Gangapuram and V. Guttena, *J. Photochem. Photobiol. B: Biol.*, **178**, 330 (2017); https://doi.org/10.1016/j.jphotobiol.2017.11.010.
11. Y. Park, J. Yoo, B. Lim, W. Kwon and S.W. Rhee, *J. Mater. Chem. A Mater. Energy Sustain.*, **4**, 11582 (2016); https://doi.org/10.1039/C6TA04813G.
12. X. Li, M. Rui, J. Song, Z. Shen and H. Zeng, *Adv. Funct. Mater.*, **25**, 4929 (2015); https://doi.org/10.1002/adfm.201501250.
13. J. Zhou, H. Zhou, J. Tang, S. Deng, F. Yan, W. Li and M. Qu, *Mikrochim. Acta*, **184**, 343 (2017); https://doi.org/10.1007/s00604-016-2043-9.
14. H. Zhu, X. Wang, Y. Li, Z. Wang, F. Yang and X. Yang, *Chem. Commun.*, 5118 (2009); https://doi.org/10.1039/b907612c.
15. Y. Zhang, Y. Wang, X. Feng, F. Zhang, Y. Yang and X. Liu, *Appl. Surf. Sci.*, **387**, 1236 (2016); https://doi.org/10.1016/j.apsusc.2016.07.048.
16. R. Bandi, N.P. Devulapalli, R. Dadigala, B.R. Gangapuram and V. Guttena, *ACS Omega*, **3**, 13454 (2018); https://doi.org/10.1021/acsomega.8b01743.
17. R. Bandi, B.R. Gangapuram, R. Dadigala, R. Eslavath, S.S. Singh and V. Guttena, *RSC Adv.*, **6**, 28633 (2016); https://doi.org/10.1039/C6RA01669C.
18. X. Sun, J. He, S. Yang, M. Zheng, Y. Wang, S. Ma and H. Zheng, *Bol. Biol.*, **175**, 219 (2017).
19. H. Liu, T. Ye and C. Mao, *Angew. Chem. Int. Ed.*, **46**, 6473 (2007); https://doi.org/10.1002/anie.200701271.
20. D. Sun, R. Ban, P.H. Zhang, G.H. Wu, J.R. Zhang and J.J. Zhu, *Carbon N. Y.*, **64**, 424 (2013); https://doi.org/10.1016/j.carbon.2013.07.095.
21. L. Tian, D. Ghosh, W. Chen, S. Pradhan, X. Chang and S. Chen, *Chem. Mater.*, **21**, 2803 (2009); https://doi.org/10.1021/cm900709w.
22. Y.H. Yuan, Z.X. Liu, R.S. Li, H.Y. Zou, M. Lin, H. Liu and C.Z. Huang, *Nanoscale*, **8**, 6770 (2016); https://doi.org/10.1039/C6NR00402D.
23. A. Sachdev and P. Gopinath, *Analyst*, **140**, 4260 (2015); https://doi.org/10.1039/C5AN00454C.
24. Z.Q. Xu, J.Y. Lan, J.C. Jin, T. Gao, L.L. Pan, F.L. Jiang and Y. Liu, *Colloids Surf. B Biointerfaces*, **130**, 207 (2015); https://doi.org/10.1016/j.colsurfb.2015.04.012.

Received: 5 February 2018 | Revised: 5 August 2018 | Accepted: 7 August 2018

DOI: 10.1002/kin.21214

ARTICLE

WILEY

Synthesis, kinetics, and mechanism of bromophenols by *N*-bromophthalimide in aqueous acetic acid

Birla Anjaiah | Kethavath Prameela | Pabba Srinivas | Kamatala Chinna Rajanna

Department of Chemistry, Osmania University, Hyderabad, India

Correspondence
Kamatala Chinna Rajanna, Department of Chemistry, Osmania University, Hyderabad 500 007, India.
Email: kcrajannaou@yahoo.com

Abstract

The kinetics and mechanism of bromination of phenol and its substituents, viz. 4-chlorophenol, 4-bromophenol, 4-methylphenol, and 4-methoxyphenol by *N*-bromophthalimide (NBP) in the presence of mercuric acetate in the temperature range of 303–318 K in aqueous acetic acid medium have been investigated. The reaction follows first-order dependence on [NBP] and fractional order dependence of rate on [Phenol]. The activation parameters have been evaluated, and based on the observed kinetic results the probable mechanism has been proposed. Observed kinetic features and Hammett's reaction constant (ρ) suggests that bromination occurs through electrophilic substitution of bromonium ion (Br^+) into the aromatic ring in the transition state. Large negative entropy of activation values probably suggests the rigid nature of transition state.

KEYWORDS

bromination, kinetics, *N*-bromophthalimide, phenols

1 | INTRODUCTION

Bromination of aromatic compounds received evergreen interest for the past several decades, because a large numbers of brominated aromatics are used as key intermediates or precursors during the synthesis of agrochemicals, pharmaceuticals, and organometallic compounds.[1–5] In the earlier years, molecular bromine was the most commonly used reagent to achieve bromination. But this reagent is not only toxic but also hazardous and releases corrosive HBr as the side product. If due care is not taken during its use, skin burns may occur. To overcome these issues, a "brominating mixture (bromate–bromide reagent)" is being used along with mineral acid for the in situ generation of either molecular bromine or tribromide ion (Br_3^-) to afford bromination. However, these methods are also associated with the excess of unused acid and HBr which will be sent into the laboratory/industrial wastes.[6] With a view to overcome toxicity issues ,considerable attention has been focused on N-halo compounds (>N–X)[7–12] for halogenation and oxidation due to their ability to act as a source of halonium cations (X^+), and hypohalite (OX^-) species. During the past several decades, *N*-bromocompounds, such as *N*-bromosuccinimide (NBS), *N*-bromoacetamide, and *N*-bromophthalimide (NBP) are most commonly used in bromination reactions, which could prevent the toxicity and acid waste.[7–12] However, in recent past, NBP is preferred over NBS owing to its high stability. A perusal of literature shows few interesting reports on oxidation kinetics,[13] but not many reports are available on the potential application of NBP as a brominating agent. Nevertheless, in a recent publication we have studied NBP triggered bromination of aromatic compounds in the presence of aqueous acetic acid. Reaction kinetics indicated first order in [NBP] and zero order in [Anisole]. The reactions afforded very good yields of corresponding bromo derivatives under kinetic conditions. The mechanism of the reaction is explained through the formation of acetyl hypobromite due to the interaction of NBP and acetic acid, which in turn reacts with anisole to afford bromo derivative of anisole.[14] Encouraged by these results, we have taken up the synthesis of bromophenols by NBP. To gain an insight into the mechanistic aspects, we have studied the kinetics of bromination of phenols using NBP in aqueous acetic acid (Scheme 1).

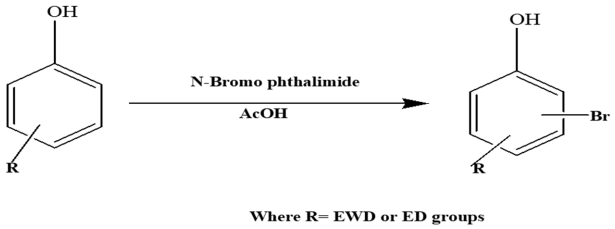

SCHEME 1 Bromination of Phenols using N-Bromo phthalimide (where EWG is electron-withdrawing, EDG is electron-donating group)

2 | EXPERIMENTAL

The reagents used in this study were obtained from Avra (Hyderabad, India), E-Merck (Mumbai, India), or Sigma Aldrich (Hyderabad, India). Acetic acid was refluxed with chromic oxide and acetic anhydride for 6 h and then fractionally distilled according to the literature procedure.[15] All aqueous solutions were prepared in doubly distilled water. Freshly prepared NBP solution was used throughout the experimental studies, even though NBP was stable enough for a couple of days. All aqueous solutions were prepared in doubly distilled water. The NBP content was estimated iodometrically using standard solution of sodium thiosulfate ($Na_2S_2O_3$) at starch end-point. The concentration of NBP was calculated using the following stoichiometric equation:

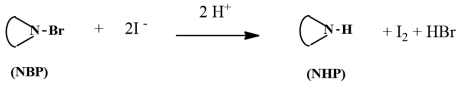

$$I_2 + 2Na_2S_2O_3 \rightarrow 2\ NaI + Na_2S_4O_6$$

2.1 | General procedure for conventional synthesis of bromoaromatic compounds using NBP

A centimolar (0.01 mol) organic substrate, 0.01 mol of NBP, and about 0.002 mol $Hg(OAc)_2$ and solvent (AcOH) were taken in a previously cleaned round bottom flask and stirred for about 9–12 h at room temperature. After completion of the reaction, as confirmed by TLC, the reaction mixture was treated with $NaHCO_3$ solution, followed by the addition of ethyl acetate. The organic layer was separated, dried over Na_2SO_4 and evaporated under vacuum, purified with column chromatography to get a pure bromo product in good yield (Table 1).

2.2 | Stoichiometry and product analysis

The stoichiometry of the reaction was determined by taking known excess of [NBP] over [Phenol] in aqueous acetic acid media at desired temperature. The progress of the reaction was followed by the iodometric method, as reported by us earlier.[13,14] The unreacted [NBP] in the aliquots of reaction mixture was estimated periodically till a constancy in the titer value is obtained. Final analysis indicated that the reactant ratio [NBP]: [Phenol] was found to be 1:1. Physical data and characteristic IR and UV spectroscopic data revealed that the products of bromination for phenol, 4-chlorophenol, 4-bromophenol 4-nitrophenol, 2-hydroxy benzoic acid, 1-naphthol, and 1-naphthylamine were 4-bromo phenol (major), 2-bromo phenol (minor), 2-bromo-4-chloro phenol, 2,4-dibromophenol, 2-bromo-4-nitro phenol, 5-bromo-2-hydroxy benzoic acid, 2-bromo-1-naphthol, 2-bromo-1 -naphthylamine, 1-bromo-2-naphthol.

Spectroscopic data for certain products are as follows:

1. *4-Bromophenol:* ^{1}H NMR (300 MHz, CDCl3) δ 5.42 (s, ^{1}H), 6.72 (dm, J = 8.9, 2H), 7.32 (dm, J = 8.9, 2H); ESI-MS m/z = 173.
2. *2-Bromophenol:* ^{1}H NMR (300 MHz, CDCl3) δ 5.5 (s, 1H), 6.74 (d, 2H), 7.35 (d, 2H); ESI-MS m/z = 173.
3. *2-Bromo-4-chlorophenol*: ^{1}H NMR (300 MHz, $CDCl_3$) δ 5.56 (s, 1H), 6.95 (d, J = 8.7, 1H), 7.19 (dd, J = 8.7, 2.4, 1H), 7.46 (d, J = 2.4, 1H); ESI-MS m/z = 208.
4. *2-Bromo-4-nitrophenol:* ^{1}H NMR(300 MHz, $CDCl_3$) δ ppm: 6.20 (s, br, 1H), 7.13 (d, J = 9.0, 1H), 8.16 (dd, J = 9.0, 2.6, 1H), 8.44 (d, J = 2.6, 1H); ESI-MS m/z = 219 (M+1).

TABLE 1 Bromination of aromatic compounds by *N*-bromophthalimide (reaction time: 9–12 h)

Entry	Substrate	Product	Yield (%)
1	Phenol	4-Bromo phenol(major)	81
		2-Bromo phenol(minor)	16
2	4-Chlorophenol	2-Bromo-4-chloro phenol	75
3	4-Bromophenol	2,4-Dibromophenol	79
4	4-Nitrophenol	2-Bromo-4-nitro phenol	75
5	2-Hydroxy benzoic acid	5-Bromo-2-hydroxy benzoic acid	75
6	1-Naphthol	2-Bromo-1-naphthol	82
7	1 -Naphthylamine	2-Bromo-1 -naphthylamine	83
8	2-Naphthol	1-Bromo-2-naphthol	84
9	2 -Naphthylamine	1-Bromo-2-naphthylamine	91

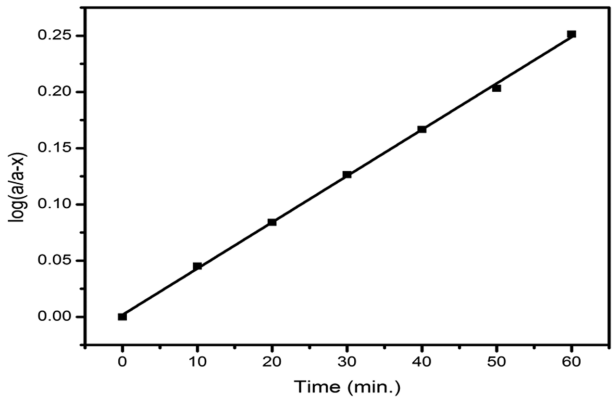

FIGURE 1 Order in [NBP] in the bromination of phenol. [NBP] = 1.33×10^{-3} mol dm^{-3}; [Phenol] = 2.66×10^{-2} mol dm^{-3}; [HOAc] = 50% v/v [$Hg(OAc)_2$] = 2×10^{-3} mol dm^{-3}; Temp = 308 K

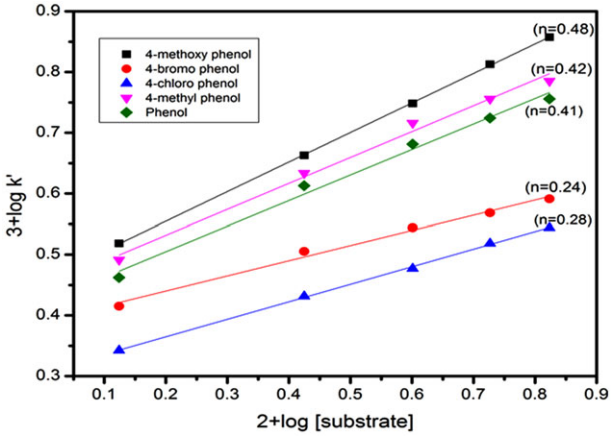

FIGURE 2 Effect of [Substrate] on k' in the NBP–phenols reaction. [NBP] = 1.33×10^{-3} mol dm^{-3}; [$Hg(OAc)_2$] = 2×10^{-3} mol dm^{-3}; [HOAc] = 50% v/v; Temp = 308 K [Color figure can be viewed at wileyonlinelibrary.com]

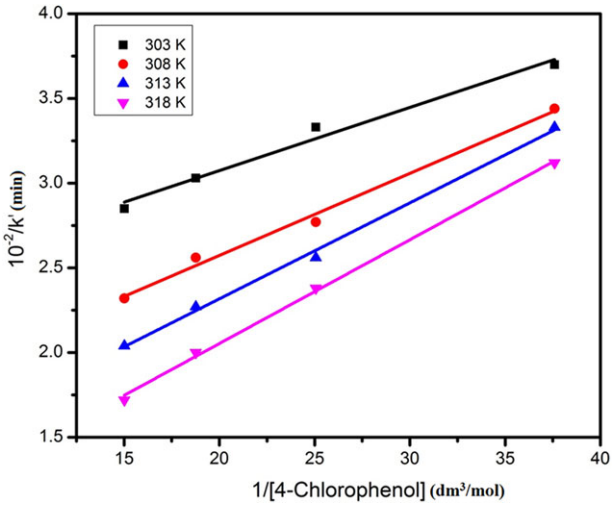

FIGURE 3 Effect of [4-chloro phenol] on k' in bromination of 4-chloro phenol–NBP reaction at different temperatures and search for complex formation: kinetic evidence. [NBP] = 1.33×10^{-3} mol dm^{-3}; [HOAc] = 50% v/v; [$Hg(OAc)_2$] = 2×10^{-3} mol dm^{-3} [Color figure can be viewed at wileyonlinelibrary.com]

5. *1-Bromo-2-naphthol:* ^{1}H NMR (300 MHz, $CDCl_3$): δ 8.04 (d, J = 8.5 Hz, 1H,), 7.76 (dd, J = 8.5 Hz, 2H), 7.61–7.56 (m, 1H), 7.43–7.38 (m, 1H), 7.27 (d, J = 8.5 Hz, 1H), 5.93 (s, 1H,) ESI-MS m/z = 221.
6. *5-Bromo-2-hydroxybenzoic acid:* ^{1}H NMR (300 MHz, CDCl3): δ 6.92 (d, J = 8.9, 1H), 7.60 (dd, J = 8.9, 2.5, ^{1}H), 8.03 (d, J = 2.5, ^{1}H), 10.39 (s, br, ^{1}H); ESI-MS m/z = 216.

3 | KINETIC METHOD

The kinetic method following the progress of the reaction is also same as that reported in our earlier publications.[13,14] Mercuric acetate was used as an additive in the reaction mixture to scavenge Br^-.[13,20] But its addition did not affect the rate of reaction to any significant extent in the present kinetic studies. Kinetic observations (observed rate constant (k') values) were reproducible with an accuracy of ±5% errors.

4 | RESULTS AND DISCUSSION

All kinetic measurements were performed under pseudo–first-order conditions with at least 10-fold in excess of [Substrate] over [NBP] ([Phenol] >> [NBP]) at a constant ionic strength (μ) and temperature.

Under these conditions, the plots of $\log(a/(a-x))$ vs. time, passing through the origin indicated the order in [NBP] to be unity (Figure 1).

Pseudo–first-order rate constants (k') were obtained from the slopes of these plots for various substrate concentrations. Observed rate constant (k') values with the variation of [Substrate] revealed that an increase in the substrate concentration increased the rate of bromination. Order (n) in [Substrate] was found less than unity ($1.0 > n > 0$), as could be seen from the slopes of the logarithmic plot of rate constant (k') as a function of [Substrate] given in Figure 2. Further, the plots of ($1/k'$) versus (1/[Substrate]) were found linear with positive slope and intercept (Figure 3) ,suggesting adduct formation prior to the rate-limiting step.

4.1 | Reactive species and mechanism

Bromination of aromatic compounds does not require a Lewis acid catalyst and differs from the bromination of alkenes. The formation of the arenium ion results in the temporary loss of aromaticity, which has a higher activation energy compared to carbocation formation in alkenes. In other words, alkenes are more reactive and do not need to weaken the Br–Br bond. Kinetic studies of NBP bromination of phenol and substituted

phenols ,viz. 4-chlorophenol,4-bromophenol, 4-methyl phenol, and 4-methoxy phenol have been studied in the temperature range of 303–318 K to understand the nature of reactive species and there by the plausible mechanism of bromination in this study.

The diverse nature of N-halo compounds and their ability to act as sources of halonium cations and hypohalite species attained considerable importance in redox reactions. As a result, these reagents react with a wide range of functional groups affecting an array of molecular transformations. NBP possesses a highly polar N–Br bond in the lines of other its structural analogue NBS. In view of this, NBP has been reported as a good oxidizing and brominating agent by earlier workers.[21–26] Thus in aqueous acetic acid solutions, NBP may exist as free NBP, protonated NBP (i.e., $NBPH^+$), HOBr, Br^+, in the lines of its structural analogue NBS according to the following equilibria:

$$NBP + H_2O \rightleftharpoons HOBr + NHP \quad \text{(i)}$$

$$NBP + H^+ \rightleftharpoons NHP + Br^+ \quad \text{(ii)}$$

$$NBP + H^+ \rightleftharpoons (NBPH)^+ \quad \text{(iii)}$$

$$HOBr + H^+ \rightleftharpoons \left(H_2OBr\right)^+ \quad \text{(iv)}$$

To analyze and ascertain the active species, effects of various additives such as $[HClO_4]$, $NaClO_4$ may though light on the influence of [Bronstead acid], ionic strength (μ), dielectric constant (D) on the reaction rate, and there by nature of reactive species. An increase in the $[NaClO_4]$ did not alter the rate significantly, whereas acidity variation ($HClO_4$) recorded rate accelerations. A kinetic study in different compositions of binary solvent mixtures of acetic and water provided information of about the variation of dielectric constant on reaction rate. A decrease in the dielectric constant (D) (increasing acetic acid composition in a binary solvent mixture of HOAc–water) had a marginal increase in reaction rates (Table 2). Further, the plot of log k' as a function of ($1/D$) was a straight line with a positive slope ,suggesting the formation and participation of cationic species $(NBPH)^+$ (Figure 4) in the rate-limiting step, according to Amis theory, as discussed in the literature. The cationic species $(NBPH)^+$ brominates with an electrophilic attack at the ring carbon as shown in the sequence of steps in Scheme 2.

The proposed mechanism is also in accordance with the observed stoichiometry, the rate equation in consonance with the mechanism proposed is given as

$$\text{Rate} = \frac{-\text{d}\,[\text{NBP}]}{\text{d}t} = \frac{kK\,[\text{S}]\,[\text{NBP}]}{1+K\,[\text{S}]} \quad (1)$$

$$\frac{\text{Rate}}{[\text{NBP}]} = k' = \frac{kK\,[\text{S}]}{1+K\,[\text{S}]} \quad (2)$$

TABLE 2 Effect of variation of different additives on the rate of NBP bromination of phenol

Additive				
10^2 [NHP] (mol dm^{-3})	10^2 [$NaClO_4$] (mol dm^{-3})	HOAc % (v/v)	[$HClO_4$] (mol dm^{-3})	$10^3k'$ (min^{-1})
0.6	–	50	–	4.1
1.3	–	50	–	4.3
2.0	–	50	–	4.1
2.6	–	50	–	3.9
3.3	–	50	–	4.4
–	0.6	50	–	4.1
–	1.3	50	–	4.8
–	2.0	50	–	4.6
–	2.6	50	–	5.2
–	3.3	50	–	4.9
–	–	30	–	3.2
–	–	40	–	3.7
–	–	50	–	4.1
–	–	60	–	4.4
–	–	70	–	5.6
–	–	50	0.6	4.1
–	–	50	1.3	5.7
–	–	50	2.0	7.0
–	–	50	2.6	7.7
–	–	50	3.3	8.3

10^3[NBP] = 1.00 mol dm^{-3}; 10^2 [Phenol] = 1.00 mol dm^{-3}; 10^3 [$Hg(OAc)_2$] = 2.00 mol dm^{-3}; temperature = 308 K.

where k_{obs} (or) k' is the pseudo–first-order rate constant. Now rearranging Equation 2 gives

$$\frac{1}{k'} = \frac{1}{kK\,[\text{S}]} + \frac{1}{k} \quad (3)$$

According to Equation 3, Lineweaver–Burk's plot of $1/k'$ vs. 1/[S] (where S denotes the substrate) should be linear with a positive slope and intercept on the Y axis. This has been observed in the present investigation (Figure 3), supporting the proposed mechanism. From the intercepts and slopes of $1/k'$ vs. 1/[S] plots at various temperatures formation constant (K) and decomposition constant (k) was calculated.

4.2 | Computation of activation parameters

Eyring's equation was used to calculate the free energy of activation ($\Delta G^{\#}$) according to the theory of absolute reaction rates. After the suitable simplification, the free energy of activation ($\Delta G^{\#}$) could be correlated to the rate constant k as shown in the following equation:

$$\Delta G^{\#} = RT\ \ln\ (RT/Nhk) \quad (4)$$

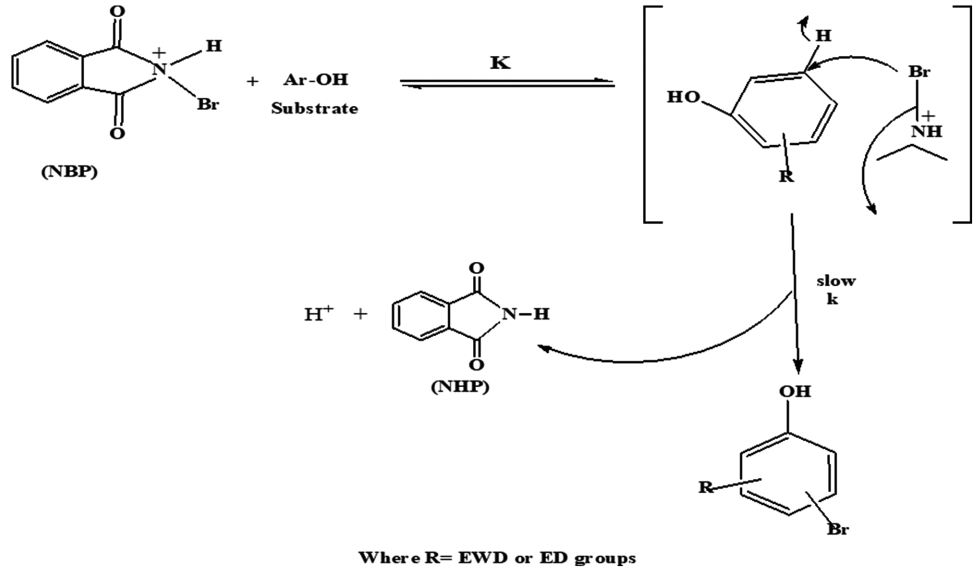

SCHEME 2 Mechanism of NBP-induced bromination of phenols

TABLE 3 Kinetic and activation parameters for the bromination of phenols by NBP

Substrate	Temperature (K)	10^3 k (dm^3 mol^{-1} min^{-1})	$\Delta G^{\neq}$ (kJ mol^{-1})	Equation with R^2	$\Delta H^{\neq}$ (kJ mol^{-1})	$-\Delta S^{\neq}$ (J K^{-1} mol^{-1})
Phenol	303	17.50	84.43			
	308	22.68	85.21		40.54	144.92
	313	30.38	85.87	$y = 144.92x + 40542$		
	318	38.93	86.63	$R^2 = 0.9992$		
	303	10.33	85.76			
4-Bromo phenol	308	13.64	86.51		49.80	118.84
	313	20.18	86.94	$y = 118.84x + 49808$		
	318	26.95	87.60	$R^2 = 0.9904$		
	303	9.87	85.88			
4-Chloro phenol	308	14.33	86.38		52.10	111.43
	313	19.44	87.03	$y = 111.43x + 52108$		
	318	27.81	87.52	$R^2 = 0.9968$		
4-Methyl phenol	303	19.52	84.16			
	308	23.89	85.07		36.54	157.33
	313	31.24	85.80	$y = 157.33x + 36545$		
	318	40.25	86.54	$R^2 = 0.997$		
4-Methoxy phenol	303	23.95	83.64			
	308	28.97	84.58		28.22	183.01
	313	34.00	85.58	$y = 183.01x + 28221$		
	318	43.07	86.36	$R^2 = 0.9977$		

[NBP] = 1.33×10^{-3} mol dm^{-3}; [$Hg(OAc)_2$] = 2×10^{-3} mol dm^{-3}; [HOAc] = 50% v/v.

where R is the gas constant, h the Plank's constant, N the Avogadro's number, and T the temperature (in the Kelvin scale). Accordingly, $\Delta G^{\#}$ values were obtained at different temperatures. Using the $\Delta G^{\#}$ values thus obtained was cast into the Gibbs–Helmholtz plot of $\Delta G^{\#}$ versus T, using the following equation from which the evaluation of enthalpy of activation ($\Delta H^{\#}$) and entropy of activation ($\Delta S^{\#}$) could be evaluated. Obtained data are compiled in Table 3.

$$\Delta G^{\#} = \Delta H^{\#} - T\Delta S^{\#} \quad (5)$$

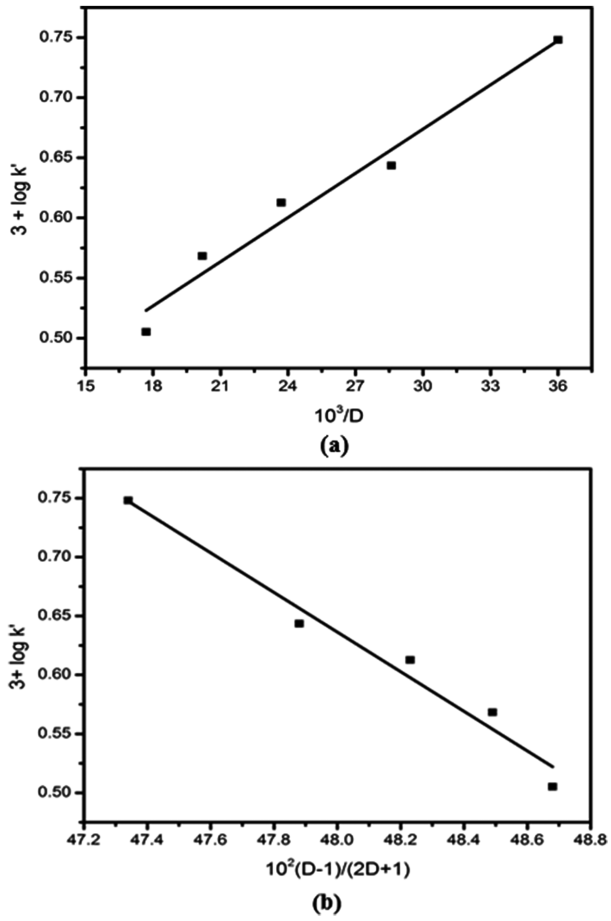

FIGURE 4 (a) Amis plot; (b) Kirkwood plot

4.3 | Computation of thermodynamic parameters involving formation constant (*K*)

Van't Hoff's isotherm was used to calculate the free energy of intermediate adduct formation (ΔG) according to the thermodynamic equilibrium concepts. According to this concept, the free energy of formation (ΔG) could be correlated to the formation constant (K):

$$\Delta G = -RT \ \ln \ (K) \tag{6}$$

Accordingly, ΔG values were obtained at different temperatures. Using the ΔG values thus obtained was cast into the Gibbs–Helmholtz plot of ΔG vs. T, using the following equation from which the evaluation of enthalpy (ΔH) and entropy (ΔS) of formation could be evaluated. Obtained data are compiled in Table 4.

$$\Delta G = \Delta H - T\Delta S \tag{7}$$

Data presented in Table 4 show the spontaneous nature of adduct, formed prior to the rate-determining step. Higher magnitude of formation constants (K) combined with the large negative entropy values of adducts, formed with NBP and

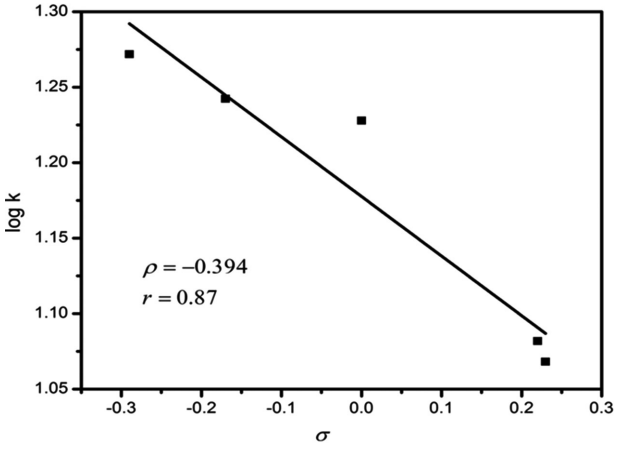

FIGURE 5 Hammett plot to explore the effect of substituent on the reaction rates in the bromination of phenol by NBP in aqueous acetic acid medium. [NBP] = 1.33×10^{-3} mol dm^{-3}; temperature = 318 K; [HOAc] = 50% v/v; [$Hg(OAc)_2$] = 2×10^{-3} mol dm^{-3}

electron-withdrawing substrates, appeared to be more rigid than their counter parts.

Hammett's Structure-Activity Relationship (HSAR): To understand the effect of phenol structure (substituent) on the rate constants (k) of the slow step, we have analyzed by Hammett's equation (Figure 5). Phenols-bearing electron-donating groups appear to be faster than those with electron-withdrawing groups. This point can also be seen from the correlation coefficient (R^2). Hammett's structure and activity relationship (SAR) for k has come out as

$$(\log k) = -0.394\sigma + 1.1776; \quad R^2 = 0.87$$

This is in accordance with Hammett's equation, $\log k = \rho\,\sigma + \log k_o$ (where $\log k$ and $\log k_o$ indicate rate constants for substituted and parent phenol, respectively). The negative magnitude of the reaction constant ($\rho = -0.3948$) shows the substitution is electrophilic in nature with a fair correlation ship ($R^2 = 0.87$). However, Hammett's SAR for formation K has been found to be

$$(\log k) = -0.9872\sigma + 14.963; \quad R^2 = 0.0231.$$

A poor correlation coefficient ($R^2 = 0.0231$) value shows that the reaction is not very much sensitive to formation constant (K) values.

Data compiled in Table 5 exhibited that the reaction constant (ρ) values are fairly large negative values ($\rho < 0$), suggesting the attack of electrophile on the aromatic ring. In addition, an increase in the temperature decreased the reaction constant (ρ) values. This trend is quantitatively

TABLE 4 Thermodynamic parameters for the bromination of phenols by NBP

Substrate	Temperature (K)	K ($dm^3\ mol^{-1}$)	$-\Delta G$ ($kJ\ mol^{-1}$)	Equation with R^2	ΔH ($kJ\ mol^{-1}$)	$-\Delta S$ ($J\ K^{-1}\ mol^{-1}$)
Phenol	303	100.84	11.62		60.71	162.29
	308	64.41	10.66			
	313	43.74	9.83	$y = -162.29x + 60719$		
	318	32.39	9.19	$R^2 = 0.9923$		
	303	212.60	13.50		91.39	257.36
p-Br Phenol	308	115.42	12.15			
	313	57.16	10.52	$y = -257.36x + 91396$		
	318	40.04	9.75	$R^2 = 0.9826$		
	303	144.39	12.52		81.10	226.76
p-Cl Phenol	308	76.10	11.09	$y = -226.76x + 81105$		
	313	48.05	10.07	$R^2 = 0.9913$		
	318	31.08	9.08			
	303	89.69	11.32		52.88	137.06
p-CH_3 Phenol	308	65.92	10.72			
	313	46.18	9.97	$y = -137.06x + 52888$		
	318	33.61	9.29	$R^2 = 0.9983$		
	303	68.22	10.63		34.90	80.01
p-OCH_3 Phenol	308	54.99	10.26			
	313	45.64	9.94	$y = -80.012x + 34907$		
	318	35.13	9.41	$R^2 = 0.9879$		

TABLE 5 Kinetic and activation parameters for the bromination of phenols by NBP

Type of Plot	Temperature (K)	Equation	R^2	Slope
log(*k*) vs. sigma	303	$Y = -0.726x - 1.817$	0.958	−0.726
	308	$Y = -0.606x - 1.703$	0.944	−0.606
	313	$Y = -0.468x - 1.580$	0.897	−0.468
	318	$Y = -0.394x - 1.46$	0.870	−0.394
log(*K*) vs. sigma	303	$Y = 0.780x + 2.057$	0.886	0.780
	308	$Y = 0.433x + 1.863$	0.672	0.433
	313	$Y = 0.124x + 1.681$	0.410	0.124
	318	$Y = 0.021x + 1.535$	0.013	0.021

represented according to the following relationship, as mentioned by Exner[27]:

$$\rho = A\left[1 - \beta/T\right] \tag{8}$$

where A is a constant and β is the isokinetic temperature. When $\beta = T$, $\rho = 0$, the effect of substituent on the rate of reaction vanishes and all the substituted compounds in a given series have the same reactivity. In this study, the isokinetic temperature (β) is found to be 336.5, which is above the experimental temperature range (300–320 K), suggesting that the importance of enthalpy factors controlling the reaction rates. Observed enthalpy of activation values, presented in Table 3, support the above conclusion as the slowest reaction exhibited high activation enthalpy (52.1 kJ/mol for p-chlorophenol) whereas the fastest reaction indicated low activation enthalpy (28.2 kJ/mol for *p*-methoxy phenol).

To verify the rate law we have been calculated rate constants (k') with the help of the rate law. The data are presented in Table 6 by taking methoxy phenol as a specific substrate.

5 | CONCLUSIONS

The NBP reaction with phenols in aqueous acetic acid afforded very good yields of corresponding bromo derivatives in 9–10 h. The reaction followed first-order kinetics in [NBP] and fractional order in [Phenol], indicating the formation of [NBP–Phenol] adduct, which was decomposed in the rate-limiting step to followed by the transfer of (Br^+)

TABLE 6 Calculated rate constants (using rate law) and experimental rate constants for the *bromination of p-methoxy phenol at various temperatures*

		k' (min^{-1})	
Temperature	**[S] (mol dm^{-3})**	**Calculated**	**Experimental**
303	0.0266	0.0154	0.0102
	0.0399	0.0175	0.0121
	0.0533	0.0187	0.0132
	0.0666	0.0196	0.0142
308	0.0266	0.0172	0.0107
	0.0399	0.0198	0.0131
	0.0533	0.0215	0.0149
	0.0666	0.0227	0.0164
313	0.0266	0.0186	0.0112
	0.0399	0.0219	0.014
	0.0533	0.0240	0.0161
	0.0666	0.0255	0.0181
318	0.0266	0.0208	0.0114
	0.0399	0.0251	0.0147
	0.0533	0.0280	0.0173
	0.0666	0.0301	0.0198

10^3[NBP] = 1.00 mol dm^{-3}; 10^3 [$Hg(OAc)_2$] = 2.00 mol dm^{-3}.

electrophile to the aromatic ring of the phenol to afford a bromo phenol derivative. Hammett's equation is in accordance with electrophilic substitution reactions.

ORCID

Kamatala Chinna Rajanna
http://orcid.org/0000-0003-0473-563X

REFERENCES

1. West RC. *CRC Handbook of Chemistry and Physics*. Boca Raton, FL: CRC Press; 1977.
2. Matthew LM, Yogesh RM, Steven M. An efficacious method for the halogenation of b-dicarbonyl compounds under mildly acidic conditions. *Tetrahedron Lett*. 2005;46:4749–4751.
3. Carreno MC, Garcia Ruano JL, Sanz G, Toledo MA, Urbano AN. *N*-Bromosuccinimide in acetonitrile: a mild and regiospecific nuclear brominating reagent for methoxybenzenes and naphthalenes. *J Org Chem*. 1995;60:532–538.
4. Wakefield BJ. *The Chemistry of Organo lithium Compounds*. Oxford, UK: Pergamon Press; 1976.
5. Vyas PV, Bhatt AK, Ramachandraiah G, Bedekar AV. Environmentally benign chlorination and bromination of aromatic amines, hydrocarbons and naphthols. *Tetrahedron Lett*. 2003;44:4085–4088.
6. Furniss BS, Hannaford AJ, Smith PWG. *Vogel's. Textbook of Practical Organic Chemistry*. 5th ed. London, UK: Thames Polytechnic; 1989.
7. Mathur NK, Narang CN. *Determination of organic compounds with N-Bromosuccinimide and Allied Reagents (Analysis of Organic Materials*. London, UK: Academic Press; 1975.
8. Lambert FL, Ellis WD, Parry RJ. Halogenation of aromatic compounds by *N*-bromo- and *N*-chlorosuccinimide under ionic conditions. *J Org Chem*. 1965;30:304–306.
9. Tanemura K, Suzuki T, Nishida Y, Satsumabayashi K, Horaguchiy T. Halogenation of aromatic compounds by *N*-chloro-, *N*-bromo-, and *N*-iodosuccinimide. *Chem Lett*. 2003;32:932–933.
10. Jagdeesh RV, Puttaswamy J. Ru(III), Os(VIII), Pd(II) and Pt(IV) catalysed oxidation of glycyl-glycine by sodium *N*-chloro-*p*-toluenesulfonamide: comparative mechanistic aspects and kinetic modelling. *Phys Org Chem*. 2008;21:844–858.
11. Gunasekaran S, Venkatasubramanian N. Oxidation of phenylmethylcarbinols by bromamine-*T*. *Proc Indian Acad Sci*. 1983;92:107–112.
12. Prabhu DV. Kinetics and re action mechanism of the controlled oxidation of some industrial alcohols by haloamines. *J Ind Chem Soc*. 2007;84:1135–1139.
13. (a) Sachdev N, Singh AK, Shrivastava A, Katre Y, Parwaz Khan AA. *Arabian J. Chem*. 2017;10:965–974; (b) Singh AK, Jain B, Negi R, Katre Y, Singh SP, Sharma VK. *Transition Met. Chem*. 2010;35:407–414; (c) Anjaiah B, Srinivas P. *J. Appl. Chem*. 2014;3:2123–2130.
14. Anjaiah B, Satish Kumar M, Srinivas P, Rajanna KC. Bromination of anisoles using *N*-bromophthalimide: a synthetic and kinetic approach. *Int J Chem Kinet*. 2015;48:98–105.
15. Orton KJP, Bradfield AE. CXXXVII—The purification of acetic acid. The estimation of acetic anhydride in acetic acid. *J Chem Soc*. 1927:983–985.
16. Heropoulos GA, Cravotto G, Screttasa CG, Steele BR. Contrasting chemoselectivities in the ultrasound and microwave assisted bromination reactions of substituted alkylaromatics with *N*-bromosuccinimide. *Tetrahedron Lett*. 2007;48:3247–3250.
17. Srinivasan C, Chellamani A. Kinetics and mechanism of bromination of anisole by *N*-bromosuccinimide. *React Kinet Catal Lett*. 1981;18:187–191.
18. Subramanya RK, Pingali AM, Monika A, Jursic BS. An efficient regioselective NBS aromatic bromination in the presence of an ionic liquid. *Tetrahedron Lett*. 2010;51:1383–1385.
19. Anjum A, Srinivas P. Kinetics and mechanistic aspects of oxidation of acetophenones by *N*-bromophthalimide in presence of mercuric acetate. *Asian J Chem*. 2005;17:553–558.
20. Pramila K, Anjaiah B, Srinivas P. Oxidation of dipeptide glycylglycine by *N*-bromosuccinimide in aqueous acetic acid medium and comparison with monomer glycine: a kinetic and mechanistic study. *Asian J Chem*. 2012;24:4671–4674.
21. Viroopakshappa J, Jagannadham V. Kinetics and mechanism of bromination of phenols by sodium bromate-sodium bisulphite reagent in water-acetonitrile mixture. *Ind J Chem*. 2004;43A:532–534.
22. Sachdev N, Singh AK, Shrivastava A, Katre Y. Kinetic and mechanistic investigations of chlorocomplex of Ru(III) and Ir(III) catalyzed oxidation of D-fructose by N-bromophthalimide in acidic medium. *J Saudi Chem Soc*. 2016;20:S357–S375.

23. Singh AK, Jain B, Reena N, Yokraj K, Singh SP. Oxidation of valine by *N*-bromophthalimide in presence of chloro-complex of Pd(II) as homogenous catalyst: a kinetic and mechanistic study. *Open Catal J*. 2009;2:12–20.
24. Alhaji NMI, Mary SSL. Kinetics and mechanism of oxidation of isoleucine by *N*-bromophthalimide in aqueous perchloric acid medium. *E-J Chem*. 2011;8:1728–1733.
25. Ghanat KJ, Katre YR, Singh AK. Kinetics of glycine oxidation by *N*-bromophthalimide in the presence of sodium dodecyl sulfate. *J Surfactants Detergents*. 2006;9:231–235.
26. Jagdish B, Balaji M, Milind U. *Int J Chem Technol Res*. 2010;2:2150–2155.
27. Exner O. On the enthalpy-entropy-relationship. *Collect Czech Chem Commun*. 1964;29:1094–1113.
28. (a) Petersen JRC. *J Org Chem*. 1964;29:3133; (b) Liu L, Guo QX. *Chem Rev*. 2001;101:673–693; (c) Cornish-Bowden AJ. *Biol Sci*. 2002;27:121–126.

How to cite this article: Anjaiah B, Prameela K, Srinivas P, Rajanna KC. Synthesis, kinetics and mechanism of bromophenols by N-Bromophthalimide in aqueous acetic acid. *Int J Chem Kinet*. 2018;1–9. https://doi.org/10.1002/kin.21214

Asian Journal of Chemistry; Vol. 28, No. 9 (2016), 1899-1902

ASIAN JOURNAL OF CHEMISTRY

http://dx.doi.org/10.14233/ajchem.2016.19729

Oxidation of Glycylglycine by $KBrO_3$ in Aqueous Acetic Acid Medium and Comparison with Monomer Glycine: A Kinetic and Mechanistic Study

PRAMEELA KETHAVATH[1], ANJAIAH BIRLA[2] and SRINIVAS PABBA[2,*]

[1]Department of Chemistry, Dr. B.R. Ambedkar Open University, Hyderabad-500 033, India
[2]Department of Chemistry, Osmania University, Hyderabad-500 007, India

*Corresponding author: Tel: +91 40 23680509; E-mail: prameelachembraou@gmail.com

Received: 16 November 2015; *Accepted*: 15 February 2016; *Published online*: 1 June 2016; AJC-17912

The kinetics of oxidation reactions of dipeptide glycylglycine (GG) by $KBrO_3$ in aqueous acetic acid medium, under the condition $[KBrO_3] << [GG]$ at different temperatures (313-323 K), to produce formic acid, ammonia, carbon dioxide and water were studied. Study of the kinetic results showed that the first order dependence in $[KBrO_3]$ and fractional order dependence in [GG]. The effect of ionic strength and [AcOH] on rate was studied and thermodynamic parameters were also calculated. Michealis-Menten type mechanism was proposed.

Keywords: Glycylglycine, Glycine, Potassium bromate, Acetic acid.

INTRODUCTION

Bromate is a hypervalent oxyanion of bromine, which is known as a versatile oxidizing agent [1-5] and brominating agent depending on reaction conditions. It oxidizes reducing agents and can be reduced to bromide and bromine. Bromate reactions with natural and synthetic gastric juices have been well documented in literature [6]. In addition, potassium bromate is a strong oxidizing agent with redox potential of 1.44 volts in acid medium [7]. Probably because of this reason bromate [Br(V)] is widely used as an oxidizing agent in synthetic as well as in analytical chemistry. Its oxidizing ability can be compared with reagents such as Ce (IV) [8], potassium iodate [9], sodium periodate [10-12], N-bromoacetamide [13-28] and N-bromosuccinimide [29-31], *etc.* have been earlier used in oxidation of various compounds.

In past several decades, potassium bromate has been widely used for the oxidation of a wide range of compounds [32-34]. Banerji and Negi [35] described the kinetics of oxidation of some aldoses and amino sugars by potassium bromate in hydrochloric acid medium. The reactions appear to proceed through the intermediate formation of bromate esters followed by the decomposition of the esters to give products. Hydrogen ion accelerated the rate of each reaction.

EXPERIMENTAL

Glycylglycine (E. Merck, analytical grade) was purified by column chromatography and used in experiment. Potassium bromate obtained from E. Merck with highest purity and analytical grade used as received, in stock solution. Acetic acid (E. Merck, analytical grade) was purified [36,37] by refluxing over chromium trioxide and acetic anhydride. The solid that separated out was filtered off and the filtrate distilled in an all glass quick fit apparatus and the fraction distilled at 118 °C was collected and used for all experiments. All other chemicals were of analytical grade.

Kinetics and measurements: The kinetic studies were carried out under pseudo-first order conditions with glycylglycine concentrations always greater than the concentration of $KBrO_3$. The progress of the reaction was monitored by estimating the unreacted concentration of $KBrO_3$ by iodometrically using freshly prepared starch as an indicator.

Stoichiometry: Stoichiometry studies were carried out under the conditions $[KBrO_3] >> [GG]$ in the presence of $Hg(OAc)_2$. The reaction was allowed to go to completion and the unreacted $KBrO_3$ was estimated iodometrically. It was found that one mole of glycylglycine required two moles of $KBrO_3$.

$$2HBrO_3 + H_2NCH_2\text{-}CONH\text{-}CH_2COOH \longrightarrow 2HCOOH + 2CO_2 + 2NH_4^+ + Br_2 + H_2O$$

Product analysis: The products of oxidation of glycylglycine were identified as HCOOH, NH_3 and CO_2. Formic acid was detected by conventional spot tests [38], while ammonia was identified by Nessler's reagent [39] and carbon dioxide was detected by gas evolution apparatus.

RESULTS AND DISCUSSION

The kinetics of oxidation of glycylglycine (GG) by $KBrO_3$ was investigated at different concentration of glycylglycine, conducted under the conditions $[KBrO_3] << [GG]$, the reaction was allowed to go for completion. The progress of the reaction was monitored by estimating the unreacted $[KBrO_3]$ at different intervals of time. The plots of $\log\frac{a}{(a-x)}$ [where 'a' and (a-x) corresponds to the concentration of $KBrO_3$ at zero time and at time 't'] *vs.* time were found to be linear passing through the origin Fig. 1 indicating first order dependence of rate in $[KBrO_3]$. From the slops of such plots pseudo-first order rate constants (k′) evaluated were independent of $[KBrO_3]$, conforming the first order dependence in $[KBrO_3]$. The rate increases with increasing in [GG].

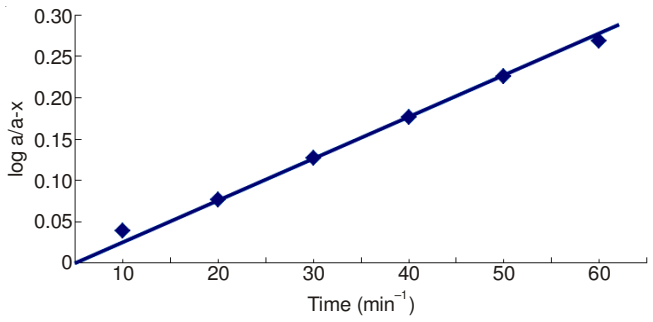

Fig. 1. Oxidation of glycylglycine by $KBrO_3$; $[KBrO_3] = 5 \times 10^{-3}$ mol dm^{-3}; $[GG] = 5 \times 10^{-2}$ mol dm^{-3}; $[Hg(OAc)_2] = 1 \times 10^{-2}$ mol dm^{-3}; [AcOH] = 10 % (v/v); Temp. = 313 K

The plot of log k′ *vs.* log [GG] (Fig. 2) was linear with n = 0.42 (r = 0.97) indicating fractional order dependence of rate on [GG]. No altering of order in glycylglycine further increasing [GG], the reaction obeying the Michealis-Menten kinetics (Table-1). The rate of oxidation of glycylglycine was not altered with the increase in ionic strength (addition of $NaClO_4$). The reaction rate was found to increase with increase in concentration of AcOH content varied by the addition of 10-25 % (v/v) AcOH in the reaction.

Comparison of rates of oxidations of glycylglycine and glycine revealed that the rate of oxidation of glycine is faster than glycylglycine (Table-2).

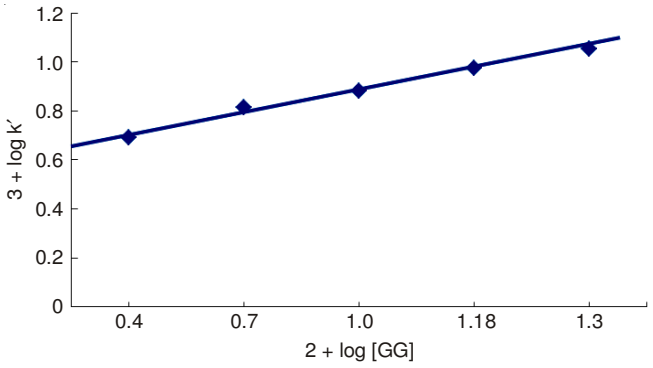

Fig. 2. Effect of [GG] on k_2 in $KBrO_3$-GG reaction; $[KBrO_3] = 5 \times 10^{-3}$ mol dm^{-3} ; Temp. = 313 K

TABLE-1
ORDER IN [GG] IN THE OXIDATION OF GLYCYLGLYCINE BY $KBrO_3$ IN AQUEOUS ACETIC ACID MEDIUM
$[KBrO_3] = 5 \times 10^{-3}$ mol dm^{-3}; $[Hg(OAc)_2] = 1 \times 10^{-2}$ mol dm^{-3}; Temp. = 313 K; [AcOH] = 10 % (v/v)

$10^2 \times$ [GG] (mol dm^{-3})	k' $\times 10^3$ min^{-1}	2 + log [GG]	3 + log k'
2.5	4.9	0.40	0.690
5.0	6.5	0.70	0.813
10.0	7.6	1.00	0.881
15.0	9.4	1.18	0.973
20.0	11.2	1.30	1.053

TABLE-2
COMPARISON OF RATE OF OXIDATION OF GLYCYLGLYCINE WITH THAT OF GLYCINE
$[KBrO_3] = 5 \times 10^{-3}$ mol dm^{-3}; $[Hg(OAc)_2] = 1 \times 10^{-2}$ mol dm^{-3}; [AcOH] = 10 % (v/v); Temp. = 313 K

$10^2 \times$ [GG] (mol dm^{-3})	$10^3 \times$ k' (min^{-1})	$10^2 \times$ [Glycine] (mol dm^{-3})	$10^3 \times$ k' (min^{-1})
2.5	4.9	2.5	8.6
5.0	6.5	5.0	10.8
10.0	7.6	10.0	11.9
15.0	9.4	15.0	14.5
20.0	11.2	20.0	17.8

The kinetic study of the reaction is studied at different temperature from 313 to 323 K. The substance concentration was changed at each temperature to follow Michealis-Menten kinetics. To determine the activation parameters, the reactions were carried out at different temperatures. Using the Arrhenius equation the activation energies (E_a) were calculated and from these values thermodynamic parameters were evaluated for the rate limiting step have been computed as follows:

Reactive species and mechanism: Potassium bromate exists in following forms in acetic acid solution *viz.*, BrO_3^- and $HBrO_3$. The possibility of BrO_3^- as the reactive species is ruled out in the present investigation as observed, that increasing the ionic strength results no change in the rate of oxidation. As the reaction were conducted in the presence of excess of $Hg(OAc)_2$, which eliminates Br^+ *via* complexation, thus any possible oxidation due to Br_2 is eliminated. Therefore in the present investigation $KBrO_3$ quickly protonated [40-45] to produce $HBrO_3$ is acting as a reactive species in the oxidation of glycylglycine and glycine using $KBrO_3$ in acetic acid medium. It supported by the acetic acid effect data on rate of the oxidation. Increases in the acetic acid content increases in the rate of oxidation increases.

$$H^+ + BrO_3^- \underset{}{\overset{K_P}{\rightleftharpoons}} HBrO_3$$

Glycylglycine exists as Zwitterions, cation, anion and neutral molecule depending on the pH of the medium [46-49].

Under the experimental conditions (pH > 3.4) zwitterion form of glycylglycine is supposed to be the reactive species of glycylglycine. Addition of olefinic monomer such as acrylamide or acrylonitrile did not induce polymerization confirming the absence of free radicals in the reaction mixture.

The first order dependence of rate on $[KBrO_3]$ and fractional order dependence on [GG] suggest that the reaction might occur *via* the formation cyclic bromate ester and in the slow rate determining step it dissociate to give final products. On

Proposed mechanism:

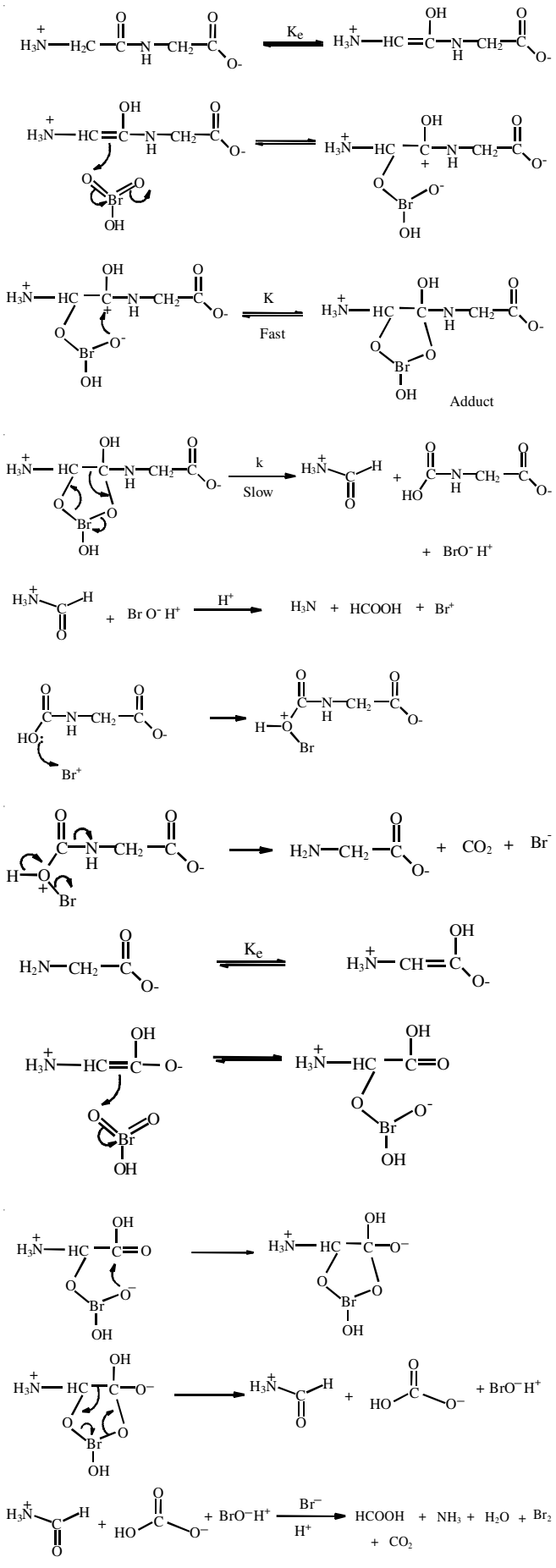

the basis of observed kinetics results, products of oxidation and above discussion, the reaction of oxidation of glycylglycine by $KBrO_3$ may be written as:

$$2HBrO_3 + H_2NCH_2\text{-}CONH\text{-}CH_2COOH \longrightarrow 2HCOOH + 2CO_2 + 2NH_4^+ + Br_2 + H_2O$$

The proposed mechanism is also in accordance with the observed stoichiometry, the rate equation in consonance with the mechanism proposed is given as:

$$\text{Rate} = \frac{-d[KBrO_3]}{dt} = \frac{kK[GG][KBrO_3]}{1 + K[GG]} \quad (1)$$

$$\frac{\text{Rate}}{[KBrO_3]} = \frac{kK[GG]}{1 + K[GG]} \quad (2)$$

Reciprocal of eqn. 2 yields:

$$\frac{[KBrO_3]}{\text{Rate}} = \frac{1}{Kk[GG]} + \frac{1}{k} \quad (3)$$

According Lineweaver Burk's plot of $10^{-3}/k_2$ *vs.* 1/[GG] should be linear with positive slope and intercept on Y-axis. This has been observed in the present investigation (Fig. 3), supporting the proposed mechanism. From the intercepts and slopes of $[KBrO_3]$/rate *vs.* 1/[GG] plots at various temperatures activation parameters (Table-3) were calculated.

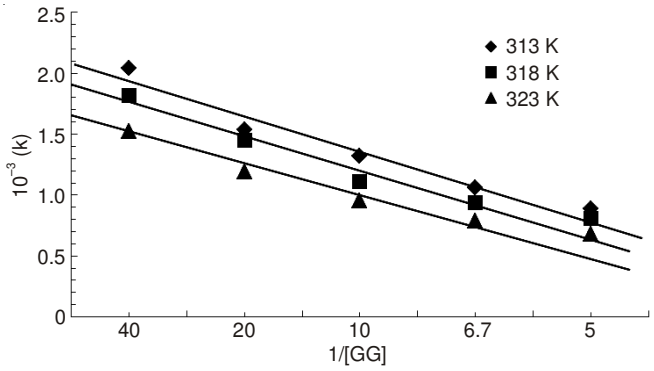

Fig. 3. Lineweaver Burk's plot of $10^{-3}/k_2$ *vs.* 1/[GG]

TABLE-3
ACTIVATION PARAMETERS FOR THE OXIDATION OF GLYCYLGLYCINE BY $KBrO_3$

Substrate	E_a (kJ mol^{-1})	$\Delta H^{\#}$ (kJ mol^{-1})	$\Delta G^{\#}$ (kJ mol^{-1})	$\Delta S^{\#}$ (J mol^{-1} K^{-1})
Glycylglycine	99.6	97.1	113.6	-52.7
Glycine	94.7	92.1	122.2	-96.1

Comparison of rates of glycylglycine-$KBrO_3$ reaction with glycine-$KBrO_3$ reaction revealed that the rate of oxidation is faster in case of glycine (Table-2). The difference of reaction rates may be due to the (i) increased distance between the functional groups, which result in weaker electrostatic effects (ii) glycylglcine (pK_1 3.2 and pK_2 8.2) is weaker both as an acid and a base when compared to glycine (pK_1 2.4 and pK_2 9.8). Thus the oxidation of dipeptide glycylglycine is expected to be slower than the monomer, which is observed in the present study. Similar observations were also made in the oxidation of glycylglycine by other oxidants like, NBS [50], Ce^{4+} [51], PMS [52], CAT [53], BAB [54], Mn(III) [55], BAT [56] and NBP [57].

REFERENCES

1. B. Tamami and M.A.K. Zarchi, *Eur. Polym. J.*, **31**, 715 (1995).
2. P.M. Pujari and P.J. Banerjee, *Chem. Soc. Dalton Trans.*, 1015 (1983).
3. F.S. Burgos, M. del Mar Graciani, E. Munoz, M.L. Moya, M.J. Capitan, M. Galan and C.D. Hubbard, *J. Solution Chem.*, **17**, 653 (1988).
4. S.B. Jonnalagadda and M.N. Shezi, *J. Phys. Chem. A*, **113**, 5540 (2009).
5. C.S. Reddy and P.S. Manjari, *Indian J. Chem.*, **49A**, 418 (2010).
6. J.D. Keith, G.E. Pacey, J.A. Cotruvo and G. Gordon, *Toxicology*, **221**, 225 (2006).
7. W.A. Latimer, Oxidation Potential, Prentice-Hall, New York, edn 2, p. 56 (1952).
8. A.K. Singh and U. Kushwaha, *Flora and Fauna*, **13**, 215 (2007).
9. A.K. Singh and U. Kushwaha, *Flora and Fauna*, **14**, 347 (2008).
10. A.K. Singh and J.P. Pachauria, *Asian J. Chem.*, **5**, 1145 (1993).
11. U. Kushwaha and A.K. Singh, *Rev. Inorg. Chem.*, **2010**, 30- 3.
12. U. Kushwaha, A.K. Singh and A. Singh, *Asian J. Chem.*, **24**, 2373 (2012).
13. B. Shah and K.K. Banerji, *J. Chem. Soc., Perkin Trans. 2*, 33 (1983).
14. B. Singh, A.K. Singh and A. Singh, *Indian J. Chem.*, **50A**, 650 (2011).
15. S. Srivastava, S. Srivastava, S. Singh, Parul and A. Jaiswal, *Bull. Catal. Soc. India*, **6**, 140 (2007).
16. S. Srivastava, K. Singh, M. Shukla and N. Pandey, *Oxid. Commun.*, **24**, 558 (2001).
17. N. Gupta, S. Rahmani and A.K. Singh, *Oxid. Commun.*, **22**, 237 (1999).
18. D.L. Kable and S.T. Nandibewoo, *Oxid. Commun.*, **21**, 396 (1998).
19. N.A. Mohamed Farook and G.A. Seyed Dameem, *E-J. Chem.*, **8**, 479 (2011).
20. R.D. Kaushik, A.K. Chaubey and P. Garg, *Asian J. Chem.*, **15**, 1655 (2003).
21. R.D. Kaushik and R.P. Amrita Dubey, *Asian J. Chem.*, **16**, 831 (2004).
22. H.X. Kong, L.-J. Li, H.G. Wei and L. Yan, J. Juan Guangpy Shi Yanshi, 20, 70 (2003).
23. S. Srivastava, V. Srivastava and A. Awasthi, *Oxid. Commun.*, **26**, 378 (2003).
24. A.K. Singh, A. Singh, R. Gupta, M. Saxena and B. Singh, *Transition Met. Chem.*, **17**, 413 (1992).
25. S. Srivastava, A. Awasthi and V. Srivastava, *Oxid. Commun.*, **26**, 426 (2003).
26. S. Srivastava, A. Awasthi and K. Singh, *Int. J. Chem. Kinet.*, **37**, 275 (2005).
27. S. Srivastava and S. Singh, *Oxid. Commun.*, **29**, 708 (2006).
28. B. Singh, D. Singh and A.K. Singh, *Int. J. Chem. Kinet.*, **20**, 501 (2004).
29. K.S. Mavalangi, Nirmala, N. Halligudi and S.T. Nandibewoor, *React. Kinet. Catal. Lett.*, **72**, 391 (2001).
30. A.K. Singh and D. Chopra, *Oxid. Commun.*, **20**, 450 (1997).
31. A.K. Singh, D. Chopra, S. Rahmani and B. Singh, *Carbohydrate Res.*, **314**, 157 (1998).
32. S. Srivastava and S. Singh, *Oxid. Commun.*, **27**, 463 (2004).
33. S. Srivastava and S. Singh, *J. Indian Chem. Soc.*, **81**, 295 (2004).
34. K.K.S. Gupta, N. Debnath and N. Bhattach, *J. Indian Chem. Soc.*, **77**, 152 (2000).
35. S.C. Negi and K.K. Banerji, *J. Org. Chem.*, **48**, 3329 (1983).
36. R. Filler, *Chem. Rev.*, **63**, 21 (1963).
37. N.K. Mathur and C.K. Narang, Determination of Organic Compounds with N-Bromosuccinimide and Allied Reagents, Academic Press, London (1975).
38. S. Srivastava, A. Kumar and P. Srivastava, *Indian J. Agric. Chem.*, **40**, 107 (2007).
39. V.B. Sharma, S.L. Jain and B. Sain, *J. Mol. Catal.*, **227**, 47 (2005).
40. E. Fagnani, C.B. Melios and L. Pezza, *Talanta*, **60**, 171 (2003).
41. F. Feigl, Spot Tests in Organic Analysis, Elsevier, Amsterdam, p. 341 (1956).
42 A. Indelli, G. Nolan Jr. and E.S. Amis, *J. Am. Chem. Soc.*, **82**, 3233 (1960).
43. M. Anbar and S. Guttmann, *J. Am. Chem. Soc.*, **83**, 4741 (1961).
44. A.F.M. Barton and G.A. Wright, *J. Chem. Soc. A*, 1747 (1968).
45. M.T. Beck, G. Rabai and G. Bazsa, *Int. J. Chem. Kinet.*, **13**, 1277 (1981).
46. M. Clugston and R. Flemming, Advanced Chemistry, Oxford University Press, p. 355 (2000).
47. C.S. Foote and J.S. Valentine, in eds.: J.F. Liebman and A. Greenberg, Active Oxygen in Chemistry, Springer, p. 153 (1995).
48. A.F. Holleman and E. Wiberg, Inorganic Chemistry, Academic Press: San Diego (2001).
49. F.L. Muller, M.S. Lustgarten, Y. Jang, A. Richardson and H. van Remmen, *Free Radic. Biol. Med.*, **43**, 477 (2007).
50. K. Pramila, A. Birla and P. Srinivas, *Asian J. Chem.*, **24**, 4671 (2012).
51. P. Kethavath and P. Srinivas, *Online J. Bio. Sci. Informatics*, **5**, 343 (2013).
52. P. Kethavath, K.N. Reddy and P. Srinivas, *J. Appl. Chem.*, **3**, 683 (2014).
53. P. Kethavath and P. Srinivas, *J. Appl. Chem.*, **2**, 1574 (2013).
54. D.S. Mahadevappa, K.S. Rangappa and N.M.M. Gowda, *Indian J. Chem.*, **20A**, 203 (1981).
55. D.K. Bhat, B.S. Sherigara and B.T. Gowda, *Bull. Chem. Soc. Jpn.*, **69**, 41 (1996).
56. T. Asha Iyengar and D.S. Mahadevappa, *Proc. Indian Acad.*, **63**, 105 (1993).
57. A. Anjum and P. Srinivas, *Asian J. Chem.*, **18**, 1 (2006).

Online Journal OF BIOSCIENCES AND INFORMATICS

Research Article **ISSN 2320-2912**

OXIDATION OF GLYCYLGLYCINE BY CERIUM (IV) IN $HClO_4$ MEDIUM AND COMPARISON WITH MONOMER GLYCINE: A KINETIC STUDY

***PRAMEELA KETHAVATH[1] and P.SRINIVAS[2]**

[1]Department of Chemistry, Dr B R Ambedkar Open University, Hyderabad, India.

[2]Department of Chemistry, Osmania University, Hyderabad-500 007, India.

Abstract:

The kinetics of oxidation reactions of dipeptide Glycylclycine(GG) by Ce(IV) in perchloric acid medium to produce formaldehyde, ammonia and carbon dioxide, under the condition[Ce(IV)]<<[GG] at different temperature (313-323 K) have been studied. The kinetics revealed that the fractional order dependence in [GG] and first order dependence in [Ce(IV)]. The rate equation was proposed. Thermodynamic perameters have been evaluated and the oxidation rate and compared with its monomer glycine.

Key words: Glycylglycine (GG), Glycine, Cerium (Ce), perchloric Acid ($HClO_4$), Sodium Perchlorate ($NaClO_4$), Acetonitrile(ACN).

***For Correspondence:** sripabba85@yahoo.co.in, prameelachembraou@gmail.com

INTRODUCTION:

The study of amino acids and peptides is one of the most exciting fields of organic chemistry. Amino acids play a significant role in a number of metabolic reactions like biosynthesis of polypeptide, protein and nucleotides. Thus the mechanism of analogous non-enzymatic chemical processes in the oxidation of amino acids is a potential area for intensive investigation[1]. However there are only few reports available for the oxidation of Glycylglycine (GG) by various organic[2,3] and inorganic[4,5] oxidants.

Tetravalent cerium[5-7] in acid solutions is a highly stable, perfectly reversible one electron oxidant, which is capable of oxidizing many inorganic and organic substances. The oxidation potential of the Cerium (IV)-Cerium (III) system is 1.70V in 1 mol dm^{-3} perchloric acid medium, 1.61V in 1 mol dm^{-3} nitric acid medium and 1.44V in 1 mol dm^{-3} sulphuric acid. From the values of these potentials it is obvious that the oxidizing capacity of cerium (IV) solutions differ from one acid to another. An extensive literature survey reveals that no report available on the oxidation kinetics of GG by Ce(IV). Hence we felt it would be worthwhile to investigate the oxidative behaviour of Ce(IV) with GG in $HClO_4$ medium to explore kinetic aspects of the reaction.

EXPERIMENTAL SECTION:

Materials and methods

For the preparation Ce(IV)oxidant, Cerium(IV) nitrate obtained from E.Merck with highest purity and analytical grade. Ce (IV)[6-7] was prepared by dissolving requisite amount of Ce (IV) compound in perchloric acid [$HClO_4$]. Freshly prepared Ce (IV) solution was used throughout the experiment. Glycylglycine (GG) (E.Merck, analytical grade) was purified by column chromatography and used in experiment. All other reagents were analytical grade and their solutions were prepared by dissolving the necessary amounts of the sample in double distilled conductivity water.

$HClO_4$ and $NaClO_4$ were used to provide required acidity and to maintain ionic strength, respectively.

Kinetics and measurements:

The kinetic studies were made under pseudo-first order conditions with [Ce(IV)] << [GG] in $HClO_4$ medium. The progress of the reaction was monitored by estimating the unreacted [Ce(IV)] at different intervals of time. The Ce (IV) content estimated Cerimetrically[8] using a ferrous sulphate and Ferroin [Fe^{+2}-1, 10-Phenantrhroline] as an indicator.

Stoichiometry and product analysis:

Under the conditions [Ce(IV)] >> [substrate] and the reaction was allowed to go for completion. The unreacted [Ce(IV)]] was estimated and it indicates that one mole of Glycylglycine needed four moles of Ce(IV)] and one mole of glycine needed two mole of Ce(IV)] to get oxidised and the stoichiometric equation is given as

$$4Ce(IV) + H_2NCH_2\text{-}CONH\text{-}CH_2COOH + 3H_2O \longrightarrow 4Ce(III) + 2HCHO + 2CO_2 + 2NH_3 + 2H^+$$

$$2Ce(IV) + H_2N\text{-}CH_2\text{-}COOH + H_2O \longrightarrow 2Ce(III) + HCHO + CO_2 + NH_3 + 2H^+$$

Formaldehyde was detected by Chromo tropic acid[9] test, while ammonia was identified by Nessler's reagent[10], and carbon dioxide was detected by gas evolution apparatus.

RESULTS AND DISCUSSIONS

The oxidation reaction of GG was conducted under the conditions [Ce(IV)] << [GG], in $HClO_4$ medium. The progress of the reaction was monitored by estimating the unreacted [Ce(IV)] at different intervals of time. The plots of log (a/a-x) Vs time (where 'a' and (a-x) corresponds to the concentration of Ce(IV) at zero time and at time't') were found to be linear passing through the origin indicating first order dependence of rate on [Ce(IV)] (Figure-1).

Fig. 1. Oxidation of glycylglycine by Ce(IV), $[Ce^{+4}] = 5 \times 10^{-3}$ mol dm^{-3} ; [GG] = 5×10^{-2} mol. dm^{-3} ; $[HClO_4] = 5 \times 10^{-1}$ mol. dm^{-3} ; Temp = 318 K

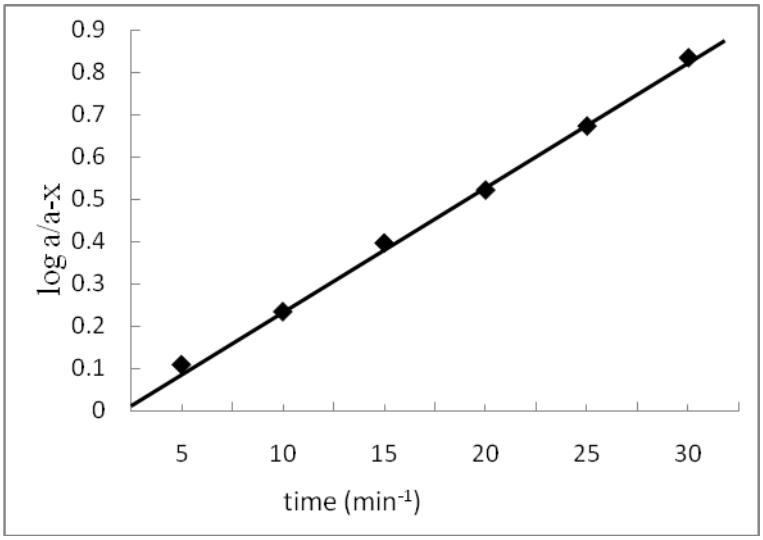

At constant [Ce(IV)], the rate increases with increase in [GG]. The plot of log k' versus log[GG] was linear(r=0.97) with a (n=0.53), indicating fractional order dependence of rate on [GG]. Order in [GG] becomes zero as [GG] is increased further, obeying the Michealis-Menten kinetics (table-1). Increasing the $[HClO_4]$, at constant ionic strength and addition of $NaClO_4$ at fixed $[H^+]$ did not affect the rate. Increase in rate was observed when the solvent composition of the medium was varied by the addition of 0-20% (v/v) Acetonitrile (ACN) (table-3). Blank experiment shows that ACN was not oxidised by Ce(IV) under the experimental conditions.

Table-1: Order in [GG] in the oxidation of GG by Ce(IV) in aqueous medium; [Ce(IV)]= 5 x 10^{-3} mol dm^{-3};Temp = 318 K

10^2 x [GG] (mol dm^{-3})	k'x 10^3 min^{-1}	2+log[GG]	3+*logk'*
2.5	2.40	0.40	0.38
5.0	3.50	0.70	0.54
10.0	4.60	1.00	0.66
15.0	5.60	1.18	0.74
20.0	7.60	1.30	0.88

Table-2: Effect of solvent (ACN) on the rate of oxidation of GG by Ce(IV) in $HClO_4$ acid medium, [Ce^{+4}] = 5 x 10^{-3} mol dm^{-3}; [GG] = 2.5 x 10^{-2} mol. dm^{-3}; [$HClO_4$] = 5 x 10^{-1} mol. dm^{-3} ;Temp = 318 K

ACN %v/v	10^3 x k' min^{-1}
00	2.4
10	2.7
15	3.5
20	4.6

Fig-2: Effect of [GG] on k′ in Ce(IV)-GG reaction: [Ce(IV)]= 5 x 10^{-3} mol dm^{-3};Temp = 318 K

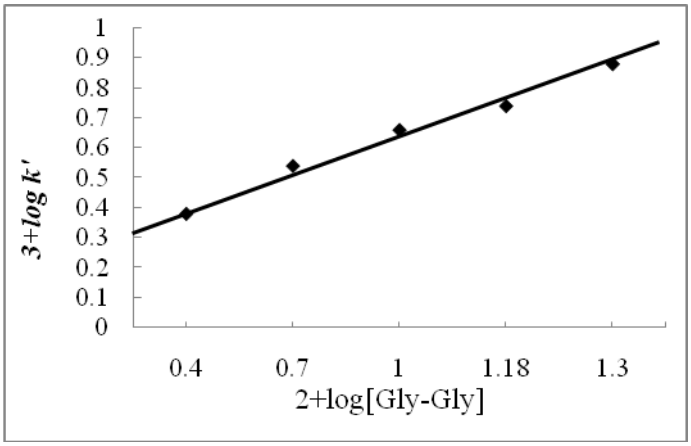

The reaction was investigated at different temperatures in the range 313-323K. The substrate concentration was varied at each temperature to Michealis-Menten kinetics (fig-3). Activation parameters for the rate limiting step have been computed as follows: E_a= 66.60 kJ mol^{-1}, $\Delta H^{\#}$ = 63.96 kJ mol^{-1}, $\Delta G^{\#}$ = 100.2 kJ mol^{-1}, $\Delta S^{\$}$ = -113.9 KJ mol^{-1}. Absence of free radicals during the course of oxidation was confirmed when no polymerization was initiated with the addition of acrylonitrile solution to the reaction mixture.

Fig-3: plot 1/k′ versus 1/[GG] at rage 313-323K

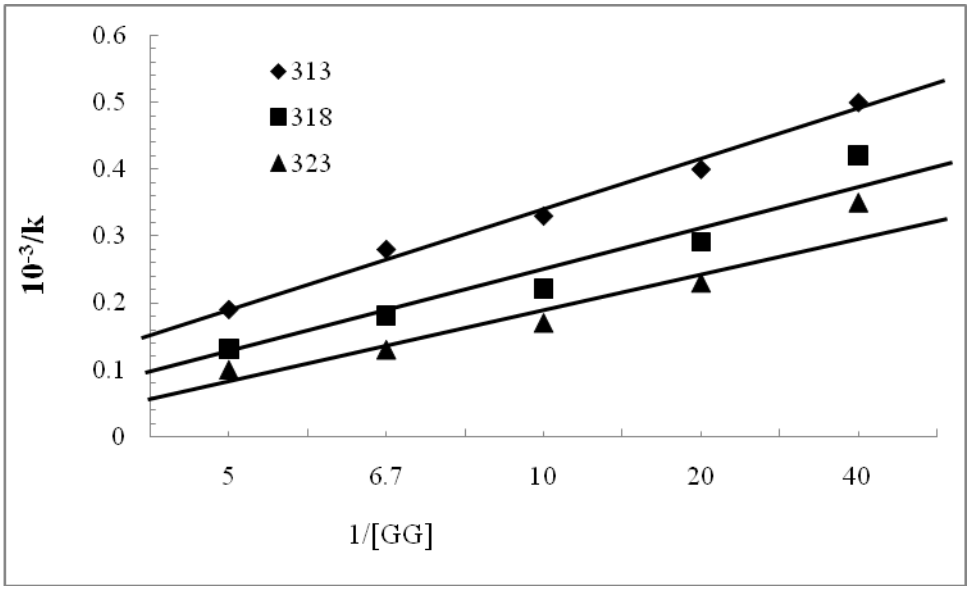

Table-3: Comparison of rate of oxidation of GG with that of glycine. [Ce(IV)] =5 x 10^{-3} mol. dm^{-3} ;[$HClO_4$] =5 x 10^{-1} mol. dm^{-3} ;Temp = 318 K

10^2 × [GG] (mol-dm^{-3})	10^3×k' (min^{-1})	10^2 × [Glycine] (mol-dm^{-3})	10^3 × k' (min^{-1})
2.5	2.4	2.5	2.85
5.0	3.5	5.0	5.30
10.0	4.6	10.0	7.60
15.0	5.6	15.0	10.40
20.0	7.6	20.0	16.20

To determine the activation parameters, the reactions were carried out at different temperatures. Using the Arrhenius equation the activation energies (E_a) were calculated and from these values thermodynamic parameters were evaluated.

Under the experimental conditions in $HClO_4$ medium, the Ce(IV) mainly exist[11] as Ce(IV), $Ce(OH)^{3+}$ and partly in polymeric forms $(Ce\text{-}O\text{-}Ce)^{6+}$, $(Ce\text{-}O\text{-}CeOH)^{+5}$ and $(HO\text{-}Ce\text{-}O\text{-}Ce\text{-}OH)^{4+}$. However, up to a concentration of 0.8 mol dm^{-3} Cerium (IV) exists in the monomeric[11] forms only. Based on the acid and ionic strength effect indicates that the activity polymeric forms of Ce(IV) is ruled out. In the present investigation Ce(IV) is supposed to be active species of in perchloric acid medium. It is also supported by the rate of reaction increases with increasing acetonitrile content in the reaction due to increasing the dipole-dipole interactions between substrate and Ce(IV) . Hence, Ce(IV) are assumed to be active species. It is also observed similarly in earlier work[12-14].

The unit order dependence of rate on [Ce(IV)] and fractional order dependence on [GG] suggest that the reaction might occur via a fast pre-equilibrium step leading to the formation of an adduct which dissociates in the slow rate determining step to give final products.

Reaction which proceed through complex formation between Cerium(IV) and substrate. More than 75% of the Cerium(IV) oxidation reactions[14] come under this mechanism. In these reactions the substrate first forms a complex with Cerium(IV) which subsequently decomposes into products, the decomposition of the complex being rate determining.

Glycylglycine[17], like the amino acids, exists as zwitterion, cation, anion and neutral molecule depending on the p^{H} of the medium. Under the experimental conditions zwitterions form of glycylclycine is supposed to be the reactive species of Glycylglycine, which gets further support from ionic strength effect. The inverse dependence of the reaction on [H^{+}] suggests that the zwitterion is reactive species taking part in the reaction. The absence of ionic strength effect on the rate limiting step.

The following mechanism was proposed,

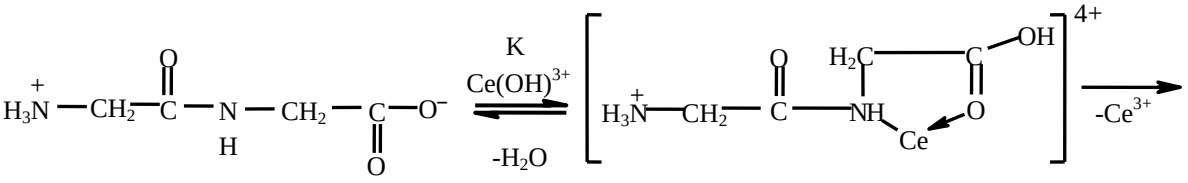

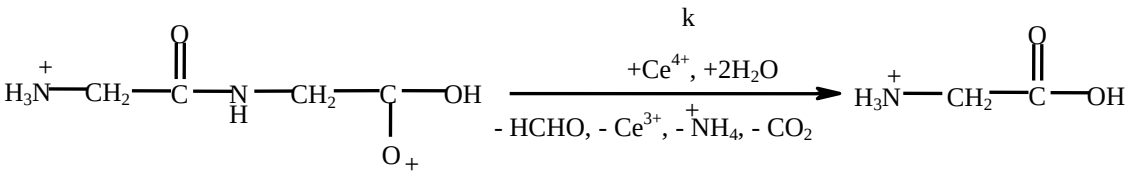

Similarly,

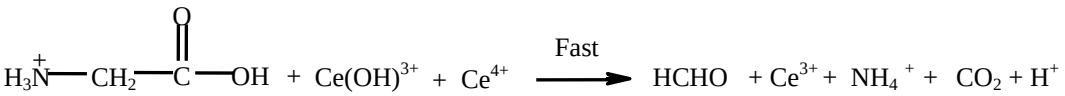

At constant ionic strength the rate law for the above mechanism can be written as

$$\text{Rate} = \frac{-d[Ce(IV)]}{dt} = \frac{kK[GG][Ce(IV)]}{1+K[GG]} \quad \ldots\ldots\ldots\ldots\ldots\ldots\ldots\ldots\ldots\ldots(1)$$

$$\frac{rate}{Ce(IV)} = \frac{kK[GG]}{1+K[GG]} \quad \ldots\ldots\ldots\ldots\ldots\ldots\ldots\ldots\ldots\ldots(2)$$

Reciprocal of equation (2) yields

$$\frac{[Ce(IV)]}{rate} = \frac{1}{Kk[GG]} + \frac{1}{k} \ldots\ldots\ldots\ldots\ldots\ldots\ldots\ldots\ldots\ldots(3)$$

According Lineweaver Burk's plot of 1/rate Vs 1/[GG] should be linear with positive slope and intercept on Y-axis. This has been observed in the present investigation and results are supporting the proposed mechanism.

Conclusion:

Comparison of rates of GG-Ce(IV) reaction with glycine-Ce(IV) reaction revealed that the rate of oxidation is faster in case of glycine (table-3). The difference of reaction rates may be due to the (i) increased distance between the functional groups, which result in weaker electrostatic effects (ii) Glycylglcine (pK_1 3.2 and pK_2 8.2) is weaker both as an acid and a base when compared to glycine (pK_1 2.4 and pK_2 9.8). Thus the oxidation of dipeptide GG is expected to be slower than the monomer, which is observed in the present study.

Reference:

1. Yathirajan, H. S; Raju, C. R; Mohana, K. N.; Sheena, S.; Padmarajaiah, N. Kinetics and Mechanism of Oxidation of L-Isoleucine and L-Ornithine Hydrochloride by Sodium N-Bromobenzenesulphonamide in Perchloric Acid Medium. Turk J Chem., 27 (2003), 571-580.

2. D.Krishna Bhat, B.Sheena Sherigara and B.Thimme Gowda, Oxidation of a Dipeptide by Electrolytically Generated Manganese(III) in Aqueous Sulfuric Acid Medium: A Kinetic and Mechanistic Study. Bull.Chem.Soc.Jpn., 69, 41 (1996).

3. Sherill. M. S., King. C.B., and Spooner, R.C., The oxidation potential of cerous-ceric perchlorates. Am. Chem. Soc., 170, 65, (1943).

4. Wylie. A. W., The potassium thorium fluorides. J. Chem. Soc., 1474 (1951).

5. Evans. M. G. and Uri. N., Photoinitiated free radical polymerization of vinyl compounds in aqueous solution. Nature, 602,166 (1950).

6. M.B. Yadav, Vijay Devra and Ashu Rani., Kinetics and mechanism of silver(I) catalyzed oxidation of valine by cerium(IV) in acid perchlorate medium. Ind. J. Chem 49A, 442 (2010).

7. D K Bhat, B S Sherigara and B T Gowda, Oxidation of 3-(3,4-dihydroxy phenyl)-L-alanine (levodopa) and 3-(3,4-dihydroxy phenyl)-2-methyl-L-alanine (methyl dopa) by manganese(III) in pyrophosphate media: Kinetic and mechanistic study. Bull. Chem. Soc.(Japan), 69, 41 (1996).

8. T A Iyenger and D S Mahadepvappa, Kinetics and Mechanism of Oxidation of Monosaccharides by Sodium-N-Bromobenzenesulfonamide in Alkaline-Medium. Indian J. Chem., 31A, 752 (1992).

9. Hardwick, T.J and Robertson, E., Ionic Species in Ceric Perchlorate Solutions. Can. J.Chem., 29, 818 (1951).

10. Heidt, L. J and Smith, M.E., Ozone and Ozonide Production and Stabilization in Water. J. Am.Chem.Soc., 70, 2476 (1948).

11. Duke, F.R. and Parchen, F.R., Kinetics of the Exchange Reaction Between Two Oxidation States of Cerium. J.Am. Chem. Soc., 78, 1540 (1956).

12. Sengupta, K.K., The sapogenin from seeds of Achyranthes aspera L. Indian Chem.Soc., 42, 725 (1965).

13. Dayal, R. and Bakore, G.V., Evalutation of organochlorine insecticide residue levels in locally marketed vegetables of Jaipur city. Indian J.Chem., 10, 1165 (1972).

14. Amjad, Z. and McAuley. A., Kinetics of the oxidation of thiourea by vanadium(V) in perchlorate media. J.Chem. Soc., Dalton Trans., 304 (1977).

15. Mehrotra, R.N. and Ghosh, S., Effect of plume geometry of recirculation flow rates in a gas injected vessel. Z. Phys. Chem. (leipzig)., 224,57 (1963).

16. M N Kumara, D Channe Gowda, A Thimme Gowda and K S Rangappa., Anodically generated manganese(III) sulphate for the oxidation of dipeptides in aqueous sulphuric acid medium: A kinetic study. J. Chem., 116(1):46 (2004).

17. Fieser L F & Fieser M, Organic chemistry (D C Heath, Boston)., 417, (1958).